

Author responses to:

Interactive comment on “Impacts of temperature and soil characteristics on methane production and oxidation in Arctic polygonal tundra” by Jianqiu Zheng et al.

We appreciate comments from both reviewers, and have used these to extensively revise our manuscript. This document includes responses to the reviewers’ comments. Finally, we have attached a comparison of the revised manuscript with the originally submitted version, at the end of these responses. These changes were widespread and substantially improved the manuscript’s readability. Note that figures have been renumbered in the revised version.

*Anonymous Referee #1*

*General Comments*

*This manuscript focuses on an important problem: the fate of the vast arctic carbon stores. It is unknown how much of this carbon will be released to that atmosphere as methane. However, we do know that emissions will be highly contingent on processes of methanogenesis and methane oxidation. How these processes will proceed in the Arctic is not entirely clear. This manuscript takes a sensible approach in proposing hypotheses that are based on better-known temperate systems. The hypotheses are then evaluated in the context of arctic soils.*

*In testing the hypotheses, the first surprising result was that methane oxidation rates did not seem to be largest near the surface (where oxygen is most abundant). Instead, these rates were largest where methane concentrations were highest. In this way, arctic soils may differ from lower-latitude soils. This manuscript also made important comparisons between the temperature sensitivities of methane oxidation and production. Understanding these temperature sensitivities is an essential step toward understanding how methane emissions will change under a warming climate.*

*Overall, I think that this manuscript has the potential to be an understandable, interesting, and useful contribution to the literature. However, as it currently stands, there are some weaknesses in the methods, and the conclusions are not entirely justified. Here are a few major points:*

*1. It does not seem that the microcosms were controlled for soil water content. This could be a major problem: the classic understanding of methanogenesis is that there is an optimum soil moisture for methane oxidation (e.g., Zhuang et al. 2004, Global Biogeochemical Cycles,*

18, GB3010). *Wouldn't soil water variation confound the results? Note that soil water can vary both across samples and, through evaporation, over time in a single sample.*

5 The incubated soils were kept at their original soil water content to best represent the field conditions in the thaw season in Barrow. These microcosms were created by placing soil in serum vials sealed with butyl rubber stoppers. Therefore, no changes in soil water content are expected during incubations, and we treated soil moisture as constant in individual samples during the incubation. Soil moisture was indeed significantly different among different samples, contributing to the variations in observed differences in methanogenesis and iron reduction rates. We developed a new Figure 1 illustrating the experimental design (discussed below), which should help clarify this point.

2. *A more rigorous statistical analysis would make the results more compelling. What are the p-values of the different fits in Figure 2? Are there any patterns in the residuals?*

15 We have fitted the data using both linear and hyperbolic models before selecting the linear model. The revised figure (now Fig. 3) includes a 95% confidence interval for the linear regression model. There was no apparent trend in the residuals from this regression.

20 3. *Regarding hypothesis 2, the bit about production exceeding consumption is not very compelling. Doesn't production have to exceed consumption? Otherwise, wouldn't concentrations would eventually go negative? Of course, consumption can exceed production if atmospheric methane is being consumed, but I don't think the authors meant to go in that direction.*

25 We consider methane consumption exceeds production when the concentration of methane in soil column is lower than the ambient level. Methane production and consumption have different temperature sensitivity, thus the net methane production in response to warming is undetermined. We clarified the second hypothesis to focus on this differential temperature sensitivity in the last paragraph of Section 1.

30 4. *The text reads as if the experiment isolated the gross rates of methane production and methane consumption. However, I was not convinced that this was the case. As far as I could tell, only the net rate was evaluated. It was not clear what effect this mismatch would have on the conclusions.*

35 The experiment isolated the gross rates of methane production and potential methane consumption. Gross production was measured by incubating samples in an anoxic N<sub>2</sub> headspace, while potential gross methane consumption was measured by incubating samples in ambient air with addition of 1% CH<sub>4</sub> headspace. We added a new Figure 1 that clarifies the experimental design, and we revised Method sections 2.2 and 2.3.

40 5. *Finally, there are numerous points (listed below) that require clarification.*

*Specific comments*

*P2, L29-30: The presence of a CH<sub>4</sub> gradient, by itself, does not suggest that methane oxidation is being underestimated.*

5

The discrepancy between high CH<sub>4</sub> concentrations in deep soil and near zero surface emissions suggest CH<sub>4</sub> oxidation can be an important factor determining surface CH<sub>4</sub> flux rates. We revised the final lines of the second introductory paragraph to better explain this idea.

10

*P3, L6: "rapid": Be more specific. Are you talking about diurnal variability, day-to-day variability, seasonal variability, something else?*

Revision: accelerated warming.

15

*Section 2.3.1: I am confused as to the number of microcosms. Is it 5x9x3 = 135? (5 soil layers x 9 replicates x 3 temperatures)? Please clarify.*

20 Yes. We started with 5x9x3 = 135 microcosms to measure CH<sub>4</sub> and CO<sub>2</sub> production. For each soil layer x temperature combination, 3 of the 9 replicates were opened to set up CH<sub>4</sub> oxidation experiments at Day 10, and additional 3 replicates were opened at Day 20. We created a new Figure 1 for the revised manuscript to better explain the workflow.

25

*Section 2.3.2: Again, I am confused as to the number of replicates. Line 3 says three replicates, line 5 says nine replicates. Also, this section is called "methane oxidation potential assay", but there are still both methanogenesis and methanotrophy going on (at least as far as I can tell). Is the argument that the effects of methanogenesis are negligible? The results would be more convincing if you explicitly make this argument.*

30

Three replicates (about 10 g soil each) were opened to reconstruct nine methane oxidation assays (about 2 g soil each). We added the new Figure 1 and explained in Section 2.4 that methanogenesis is expected to be negligible under the fully oxic conditions of the methane oxidation potential assay.

35

*Section 2.5: Several points need clarification. The text states that B<sub>methanotrophs</sub> and B<sub>methanogens</sub> were "estimated", but it does not say how they were estimated. Please clarify. The text states that V<sub>max,oxi</sub> and V<sub>measure,pro</sub> were obtained from incubations, but does not provide details. Explain how this is done. Were all incubations at all temperatures used, or was only a subset? Also, for any given incubation, how do you separate out production and consumption (since both are presumably happening*

40

*in all incubations)? What is the justification for assuming that  $R_{oxi}=R_{pro}$ ? Finally, the text states that initial CH<sub>4</sub> and O<sub>2</sub> measured concentrations were used, but don't you need a time series of these to estimate the parameters?*

5 This simple simulation for Figure 7 (now Figure 8) was performed to illustrate the increasing ratio of methanotrophs to methanogens required for a zero net CH<sub>4</sub> emission scenario at increasing temperature. Therefore, we calculated the ratio of methanotroph biomass ( $B_{methanotrophs}$ ) to methanogen biomass ( $B_{methanogens}$ ) at an equilibrium state where  $R_{oxi}=R_{pro}$ . This simulation illustrates whether the soil is going to be a CH<sub>4</sub> source or sink at  $B_{methanotrophs}$  to  $B_{methanogens}$  ratios different from these  
10 equilibrium curves. We modified Figure 8 with text illustrating the CH<sub>4</sub> sink conditions above the plotted lines, and CH<sub>4</sub> source conditions below the plotted lines.

$V_{max,oxi}$  and  $V_{measure,pro}$  were obtained from rates measured at three temperatures in soils from the FCP transition zone, as this layer exhibited highest CH<sub>4</sub> production and consumption rates. By fitting  
15 measured rates at three different temperatures with an exponential function, we further estimated the biomass ratio in response to temperature changes. Only the initial CH<sub>4</sub> and O<sub>2</sub> concentrations are needed for assessment of methane balance in the given soil. No temporal scale is included in this figure. We will clarify calculations for these curves in a revised Methods section 2.6.

20 *Section 3.2.1: Why is there apparently negligible production from the HCP permafrost soil, incubated under anoxic conditions?*

The measured CH<sub>4</sub> concentrations from HCP permafrost were mostly below the detection limit of our  
25 gas chromatograph with flame ionization detector. We believe this is mostly due to the overall low microbial activity from the HCP permafrost, also measured as CO<sub>2</sub> production.

*P13, L23-26: These sentences are a direct description of results obtained in this study. They belong in the "Results" section.*

30 We assumed zero net CH<sub>4</sub> production to demonstrate the possible uncertainties associated with temperature increase and the sensitivity to different ratios of methane producing and consuming microbes (Figure 8). This simulation is a discussion point used to support our point that more accurate representation (and measurement) of methanotrophs and methanogens biomass is needed. We clarified  
35 this simulation, as described above.

*Discussion: I am wondering if you could include a few sentences that explicitly describe how your results will effect the development of mechanistic methane models.*

40 We added a sentence to the Discussion outlining our strategy to use results from these experiments to

structure and parameterize a mechanistic model of anaerobic organic matter decomposition with greenhouse gas production.

*Technical corrections*

5 *P2, L27: "huge" is too imprecise*

We replaced "huge" with "hundred-fold."

*P2, L29: "deeper" than what?*

10 We described these depths as deeper than 20 cm per the Vaughn et al. reference.

*P3, L7 and L24: Why is it a nonlinear response to temperature "fluctuations"? Isn't it a nonlinear response to temperature? (That is, I think you should omit the word "fluctuations".)*

15 We omitted "fluctuations" in the revised manuscript.

*P3, L25: Respond more "rapidly" or more "strongly"?*

20 We replace "rapidly" with "strongly."

*P13, L4: "disparately" is the wrong word here.*

25 We revised this paragraph to remove the sentence in question.

*P13, L23-24: What is meant by "temperature profile"?*

30 This section has been re-written for clarity.

*Anonymous Referee #2*

35 *The manuscript "Impacts of temperature and soil characteristics on methane production and oxidation in Arctic polygonal tundra" of Zheng and co-authors presents results from incubation experiments of samples from two polygon centres of the arctic tundra in Alaska. The authors sectioned two cores in three layers (active layer, transition zone, permafrost) and incubated samples of these layers under either aerobic or anaerobic conditions. They measured methane (CH<sub>4</sub>) production in the anaerobic layers and CO<sub>2</sub> production and CH<sub>4</sub> oxidation in all of the layers at three different temperatures (-2\_C, 4\_C, 8\_C).  
40 Furthermore they measured low molecular weight fatty acids and ferrous iron concentrations at three*

time points of the incubation experiment and gradients of dissolved CO<sub>2</sub> and CH<sub>4</sub> concentrations at the field sites. From the data of the temperature incubation experiments they calculated Q<sub>10</sub> values for CH<sub>4</sub> production and oxidation at each depth layer at the two sampling sites.

5 *The manuscript presents potentially interesting data but the study seems not clearly focussed. The main part of the study deals with CH<sub>4</sub> production and oxidation but one of the main novel conclusions is that iron reduction is more important for the anaerobic degradation of organic matter than methanogenesis. This would be an interesting result but the methodology and data used to support this this conclusion remain unclear.*

10 *It is unclear how the authors assessed the importance of methanogenesis and iron reduction. The authors present acetate concentrations and then calculate how much of this acetate was consumed by methanogenesis and iron reduction (Fig. 8).*

*However, it remains unclear how this was done. Acetate concentrations in the soil are a function of acetate production rates e.g. by fermentation and acetate consumption rates e.g. by methanogenesis and iron reduction. Hence concentrations give no information about production rates. Furthermore, the description of the experiments and analysis is in many parts unclear (see also specific comments). It is difficult to follow the incubation experiment and in particular the CH<sub>4</sub> oxidation experiment. Samples were incubated at different temperatures to measure the temperature response of CH<sub>4</sub> oxidation, but they seem to have been also pre-incubated, but at different temperatures at the different sampling sites. This is confusing and should be clarified. One of the two hypothesis rather states current knowledge than a novel research idea. Furthermore, the aim of some of the presented approaches in the manuscript remain obscure, e.g. the "calculation of net CH<sub>4</sub> emissions" (2.5).*

25  
30 We added details for the stoichiometric calculations used for Figure 8 (now Figure 9) and present an example in the Discussion on page 13. A new Figure 1 illustrates the workflow for anoxic incubations and methane oxidation assays (see also responses to Reviewer 1).

*specific comments*

35 *P1, L23: To my knowledge, high latitude terrestrial ecosystems are a clear CH<sub>4</sub> source, even if atmospheric CH<sub>4</sub> may be oxidized in dry soils. Please rephrase.*

We rephrased this sentence in the revised manuscript to clarify the uncertainty over which soils will function as a net CH<sub>4</sub> source or sink in future high latitude ecosystems, affected by warming and associated hydrological changes.

40 *P2, L14: See comment above.*

We removed this sentence, which was redundant to the abstract.

5 *P3, L12: This might be right for the oxidation of atmospheric CH<sub>4</sub>, but for wetlands, showing substantial CH<sub>4</sub> production, this is not the case. Generally, highest CH<sub>4</sub> oxidation is found in wetlands at the aerobic/anaerobic interface, which is close to the water table.*

10 We rephrased this sentence to better distinguish between unsaturated soils and submerged (wetland) soils.

*P3, L32: This sentence is unclear. Why is additional research on CH<sub>4</sub> oxidation needed to improve estimates on CH<sub>4</sub> production? Please rephrase.*

15 We removed this sentence.

*P4, L1: Please specify the carbon decomposition pathways investigated.*

20 We rewrote this sentence to better introduce the manuscript. This manuscript does not attempt to elucidate all carbon decomposition pathways. Rather it focuses on the terminal fermentation, methanogenesis and anaerobic respiration pathways that produce CO<sub>2</sub> and CH<sub>4</sub>.

*P4, L5: This is not a hypothesis but well established textbook knowledge.*

25 We specify the hypothesis in the context of flat centered polygons and high centered polygons, which have relatively dry organic layers and wet permafrost layers, in the revised manuscript.

30 *P5 L24ff: Please clearly explain, which samples were incubated aerobically and which anaerobically. I assume the samples treated in the anaerobic chamber were also incubated anaerobically but this is not stated.*

The new Figure 1 illustrates how organic soils were incubated under oxic conditions, while soils from transition zone and permafrost were incubated under anoxic conditions.

35 *P6 L4ff: Which samples? Are this the same "microcosms" than presented in 2.3.1? and how much is ample?*

The new Figure 1 and additional experimental details added to Methods section 2.3 describe how the anaerobic incubations and methane oxidation assays were constructed.

40

*P6 L9: Why are there two different incubation temperatures for FCP and HCP? I understood from the preceding sentence that the samples were incubated at the three different temperatures -2\_C, 4\_C and 8\_C. Please clarify.*

5 The samples were incubated at three different temperatures. A subset of samples were shaken to minimize potential gas-liquid phase transfer limitations. This has been clarified in Methods section 2.4.

*P6, L20: Please cite the method for Fe<sup>2+</sup> measurements.*

10 We added a description of the Hach method 8146 assay for Fe(II) to Methods section 2.1.

*P6, L25: Table S3.*

15 Corrected to Table S1.

*P7, L3ff: The concept presented here is unclear. What is the aim of these calculations? Do the authors aim to calculate CH<sub>4</sub> emissions as stated in the header? Please clarify. Furthermore, some of the assumptions are probably not met. It is unclear why the rate of CH<sub>4</sub> oxidation should equal the rate of CH<sub>4</sub> production? This would mean zero emission of CH<sub>4</sub>. Is this likely? And finally the authors assume a certain K<sub>m</sub>-value for CH<sub>4</sub> and O<sub>2</sub> and also give a very wide range of reported K<sub>m</sub> values. It should be explained why these particular K<sub>m</sub>-values were chosen. And how would a change in the K<sub>m</sub>-values affect the calculated biomass of methanogens and methanotrophs.*

25 We rewrote this section 2.5 (now 2.6) to clarify. (Please see also comments in response to Reviewer 1). The aim of the simulation is to demonstrate the wide range of uncertainties in net methane production and impact of methanotroph to methanogen biomass ratios in response to temperature increase. We assumed zero net CH<sub>4</sub> production to help us understanding whether the soil is predicted to be a CH<sub>4</sub> source or sink. We changed Figure 7 (now Figure 8) in the revised manuscript with clear marks of CH<sub>4</sub> source and sink: CH<sub>4</sub> sink above the plotted lines, and CH<sub>4</sub> source below the plotted lines. We intentionally included a wide range of K<sub>m</sub> values used in models for this sensitivity analysis as we do not have enough information to preferably select certain K<sub>m</sub> values.

35 *P7, L19ff: It would be interesting to see the water content related to soil volume. The different depth layers show substantial differences in organic carbon concentrations, which likely are also related to substantial differences in bulk densities.*

40 A revised Figure 2 now illustrates both gravimetric water content and bulk density. We will add a plot of soil bulk density as an additional panel in Figure 1. As the reviewer suggests, high organic carbon content

usually leads to a low bulk density for Arctic soils.

*P8, L1ff: Dissolved gas concentrations should be calculated based on volume soil pore water (e.g. as  $_M$ ). Relating it to dry weight is misleading considering that gas cannot be dissolved in a solid.*

The manuscript now reports dissolved gas concentrations in micromolar units. Normalizing gas concentrations to soil mass facilitates stoichiometric comparisons with organic acids, iron, and gases produced in microcosms, although we agree it is not physically relevant.

*P8, L5: If no CH<sub>4</sub> was detected, does this indicate the oxidation of atmospheric methane in the soil? The detection limit was given as 1 ppm, which is below atmospheric concentrations.*

No. The limit of detection reflects the GC system's signal to noise properties. It does not reflect the efficiency of quantifying CH<sub>4</sub> dissolved in the soil pore water or headspace. This data can only be interpreted as no CH<sub>4</sub> produced was measured. We infer this observation is due to the low level of total microbial activity measured as CO<sub>2</sub> production.

*P8, L7: Which statistical test was used to test for significance?*

We clarified in section 3.1 that deeper soil layers in the polygon contained 5-7 fold higher concentrations of Fe(II) than surface layers.

*P8 L9ff: Better give the carbon concentrations together with the other profile data in Fig. 1. What about the carbon concentrations above 10 cm soil depth? If these are missing, a general comparison between active layer and the other samples is problematic, since generally active layer carbon concentrations are highest at the surface.*

Soil carbon concentrations were measured in the combined, homogenized core segments, reported in Table S1. Above 10 cm, the HCP and FCP cores contained mostly plant material, litter and ice (Figure 2 and Section 3.2). Since these segments have little soil, they were not considered here.

*P8, L30: What means 0 and 5 days? Were they pre-incubated for 5 days with CH<sub>4</sub>?*

*Please clearly explain in M&M.*

The new Figure 1 and revised Methods section 2.4 should clarify this experimental workflow.

*P9, L12ff: The data on the temperature response of CH<sub>4</sub> production and oxidation should not be presented only in the text of the manuscript but also as a graph or table*

as well. According to the title of the manuscript these data are the most important ones.

The new Figure 5 illustrates the temperature sensitivity of CH<sub>4</sub> production and oxidation.

5 *P9, L18ff: Please explain the meaning of the error for the Q10 values and how this was calculated.*

A revised Methods section 2.5 describes Q10 value calculations.

10 *P10, L15ff: Calculating Q10 values from rates derived from different fitting methods (linear and hyperbolic) at the respective temperatures is problematic. I suggest using only one fitting method for all of the incubation temperatures and then use these data to calculate Q10 values.*

15 *P10, L18f: Please explain how the Q10 value was estimated.*

We used linear fitting to estimate the initial production rate of CO<sub>2</sub> for Q10 calculation. A revised Methods section 2.5 describes Q10 value calculations.

20 *P10, L19f: This sentence should go to the discussion.*

Revised.

25 *P10, L23ff: Please explain in the M&M how these fatty acids were analysed.*

A short description of the organic acid analyses was added to Methods section 2.3.

30 *P10, L30: Please explain how significance tests were conducted. There seem to be no replicate analysis before day 90.*

We used paired t-test with additional technical replicates.

35 *P11, L5: please explain this approach in M&M.*

Explained in Methods section 2.3.

40 *P11, L14: Please explain how the rates were calculated. Over the whole incubation period or only for certain incubation intervals?*

Iron reduction rates were estimated by the changes in Fe(II) concentration –now explained in Methods section 2.3.

*P11, L15: How were Q10 values “estimated”?*

5

The Q10 values of iron reduction were estimated using the ratio of iron reduction rate measured at 8 degree C and -2 degree C. Please see section 2.5.

*P11, L28: This sentence is unclear. Why does lower active layer than permafrost*

10 *CH4 concentrations indicate CH4 oxidation in the active layer? Permafrost CH4 is not released from the permafrost since it is frozen. Please clarify.*

We clarify in the revised manuscript.

15 *P11, L29ff: This statement is incorrect. There are numerous studies on CH4 production and CH4 oxidation in the Arctic also showing that CH4 is produced in the anoxic soil layers and oxidized in oxic soil layers. This is an obvious fact, which likely needs no further testing if there is no evidence against it. Furthermore, differences in the temperature response of CH4 production and oxidation has been shown also for Arctic*  
20 *environments and respective studies were also cited by the authors.*

We rephrased the questions to be more specific to polygonal tundra with fine scale microtopographic features. Our data show a surprising overlap between maximum methanogenesis rates and methane oxidation potential in the transitional layer.

25

*P12, L4f: This statement is not completely correct. It is current knowledge and obvious, that CH4 production depends on both CH4 and O2 supply. Therefore, indeed CH4 oxidation depends on oxygen supply but if CH4 is present. Hence, many studies on CH4 oxidation in wetlands (including those in the Arctic) demonstrate that the*

30 *oxic/anoxic interface is the zone of most intense CH4 oxidation, which are not necessarily the aerobic surface soil layers, since there, as the authors correctly stated, low CH4 concentrations limit CH4 oxidation. Hence the soil water table is often more in- formative than the gravimetric water content for identifying the zone of maximum CH4*  
35 *oxidation.*

35

We clarify in revision that both CH<sub>4</sub> and O<sub>2</sub> diffusion can limit aerobic methane oxidation. We appreciate the reviewer’s perspective on the importance of the oxic/anoxic interface as the hotspot for aerobic CH<sub>4</sub> oxidation in wetlands. A cited review by Segers (1998) provides a valuable overview of potential methane oxidation rates as a function of distance to oxic/anoxic interface (p. 39). Average rates are highest near  
40 the water table as expected, but maximum values are on the anoxic side of the interface. However, this

distance factor explains only a small part of the variance observed in the distribution of methane oxidation potential. Therefore, other factors must influence methane oxidation potential as well.

5 We are still surprised that the maximum methane oxidation potential in flat-centered polygon soils was observed in the transition (40-50 cm) and permafrost (50-70 cm) layers –far below the near-surface water table and overlapping with areas of anaerobic methanogenesis and iron reduction. One could interpret this as a result of a fluctuating water table (as the reviewer suggests, below). However, there is no evidence for recent fluctuations in the near-surface water table at this flat center polygon, as discussed on page 12. Alternatively, we could hypothesize that the oxic/anoxic interface comprises a large part of  
10 this soil column rather than the narrow horizontal line usually drawn near the water table in conceptual diagrams. Such a broad suboxic zone would be consistent with the dissolved Fe(II) and CH<sub>4</sub> profiles show in in Figure 1. Proximity to CH<sub>4</sub> sources would be more important than proximity to the water table in this model. Future studies will be required to understand the complex O<sub>2</sub> transport mechanisms in this cold, saturated FCP soil.

15 *P12, L30f: The meaning of this sentence is unclear. Do the authors assume, that the main oxygen source in the saturated zone is from dissolved oxygen in rain water percolating through the soil and not from molecular transport through the gas phase through unsaturated pores? Please clarify?*

20 Based on the high water table of flat-centered polygons and the substantial precipitation preceding our sampling campaign, we do not expect much gas transport through unsaturated pores in this soil. We clarified this point in the Discussion.

25 *P12, L34ff: Which observations? I do not see that the survival of methanotrophs under changing redox conditions argue against highest CH<sub>4</sub> oxidation at the water table. I assume the authors mean here in situ CH<sub>4</sub> oxidation and not potential CH<sub>4</sub> oxidation measured in the laboratory. It has been shown repeatedly that highest CH<sub>4</sub> oxidation is found in the soil layer where elevated CH<sub>4</sub> concentrations overlap with oxygen. This  
30 is in soils generally close to the water table. However, if the water table fluctuates, potential CH<sub>4</sub> oxidation rates measured in the laboratory do not need to correlate with the current water table, but likely in situ CH<sub>4</sub> oxidation rates do. There is no way to aerobically oxidize CH<sub>4</sub> without the presence of CH<sub>4</sub> and oxygen.*

35 See response above.

*P13, L13F: Why should this be? Please explain.*

40 Sharp temperature gradients along unsaturated soil depth. This sentence has been removed to better focus the paragraph.

5 *P13, L20f: What is meant by “outcompete”? Methanogens and CH4 oxidizers are not competitors. I understand that it is meant that CH4 production is expected to be higher than CH4 oxidation. But why is this likely. It has been shown that even at 8\_C the potential CH4 oxidation with the current community size is 7 times higher than methanogenesis. I would rather say that it is highly unlikely that CH4 production will be higher than potential CH4 oxidation.*

10 We replaced “outcompete” with “outpace” to better represent the kinetics of these two processes. Our point in the simulation shown in Figure 7 (now Figure 8) is to illustrate the disparate effects of temperature on methanogenesis and methane oxidation activity and address model sensitivity to assumptions of half saturation rates. We believe the simulations illustrated in Figure 8 are important to illustrate the potential impact of temperature on changes in microbial population dynamics required to maintain a CH4 equilibrium.

15 *P13, L21-L29: This part of the discussion is unclear and in part speculative. The purpose of these calculations was not clearly stated in the description in the M&M section (see above) nor is it here. It might be interesting if the authors would have data on the microbial biomass of methanogens and CH4 oxidizers. But as it is now, it gives no substantial additional information.*

20 See above.

25 *P14, L1: Which incubations are referred to? The permafrost only or also the active layer?*

This refers to all incubations, including permafrost and active layer. Clarified in the Discussion.

30 *P14, L4f: To which samples is referred to here? To the FCP samples and the HCP samples?*

FCP samples. Clarified in the Discussion.

35 *P15, L5f: The described pattern was obviously not observed for the HCP in this study. What could be the differences to the cited study?*

40 We did not see evidence of cryoturbation in the HCP core used in this study. The organic layer of HCP contained much lower level of organic acids comparing to the FCP organic layer, so overall the substrate level is low.

*P14, L9f: It is obvious that organic carbon oxidation processes contribute to anaerobic CO2 production, which is the result of organic carbon oxidation. Please rephrase.*

5 We rephrased this section of the discussion to highlight the substantial contribution of anaerobic respiration from iron reduction to CO2 production, compared to methanogenesis and fermentation that also produce CO2.

10 *P14, L12ff: This sentence should be split into two. Furthermore, the information content is limited. It seem obvious that CH4 isotopes are consistent with either acetoclastic methanogenesis or hydrogenotrophic methanogenesis since these are the mayor pathways of methanogenesis. Does this sentence mean that acetate is mainly oxidized via methanogenesis and not via iron reduction? This seems to contradict the first sentence of this paragraph.*

15 This long sentence was intended to explain our assumption of acetoclastic methanogenesis for our simulation. However, it introduced needless confusion through the remote possibility of complex isotope fractionation caused by syntrophic organic acid oxidation coupled to hydrogenotrophic methanogenesis. We deleted this complex sentence for clarity.

20 *P14, L15: These calculations should be described in the M&M section. The acetate concentrations are rising during the incubations. Hence, there is a net production over time. But how was gross acetate production calculated? This is not possible from the concentration data alone. The data presented in Fig. 8 are not comprehensible.*

25 We clarified these calculations in Section 2.6 and added an example to help interpret Figure 8 (now Figure 9). The net production of acetate over time was measured. The consumption of acetate was calculated based on the stoichiometry of iron reduction and methanogenesis utilizing acetate as electron donor. Thus, we estimated the overall gross production of acetate.

30 *P14, L29ff: This last paragraph gives the current and well-established view of organic matter decomposition in wetlands. It might fit to the introduction but is not needed at the end of the discussion. The relative importance of iron reduction versus methanogenesis is an interesting issue but the data collected here does not allow a meaningful comparison of these two processes. Hence, I rather suggest omitting Fig. 9.*

35 We believe the conceptual Figure 9 (now Figure 10) will help readers to integrate the numerous processes discussed in this paper. Therefore, we prefer to keep it.

40 *Fig 5: Please show in the panels which samples were incubated aerobically and which*

*anaerobically.*

The new Figure 1 clarifies this experimental design.

5 *Fig. 8: Acetate concentrations rather than acetate production are presented in this Figure. Please rephrase.*

We revised the Figure 9 legend to described changes in acetate concentrations associated with production and consumption processes.

10

*Fig S1: This figure is unclear. What do the red circles mean?*

The circles show the combined soil sections used for incubations. The Figure S1 legend has been revised to explain this point.

15

## Changes to Manuscript

### Impacts of temperature and soil characteristics on methane production and oxidation in Arctic **polygon** tundra

5 Jianqiu Zheng<sup>1</sup>, Taniya RoyChowdhury<sup>1,2</sup>, Ziming Yang<sup>3,4</sup>, Baohua Gu<sup>3</sup>, Stan D. Wullschleger<sup>3,5</sup>, David E. Graham<sup>1,5</sup>

<sup>1</sup> Biosciences Division, Oak Ridge National Laboratory, Oak Ridge, Tennessee, USA

<sup>2</sup> Now at Department of Environmental Science & Technology, University of Maryland, College Park, Maryland, USA

<sup>3</sup> Environmental Sciences Division, Oak Ridge National Laboratory, Oak Ridge, Tennessee, USA

10 <sup>4</sup> Now at Department of Chemistry, Oakland University, Rochester, Michigan, USA

<sup>5</sup> Climate Change Science Institute, Oak Ridge National Laboratory, Oak Ridge, Tennessee, USA

Correspondence: David E. Graham ([grahamde@ornl.gov](mailto:grahamde@ornl.gov))

15 This manuscript has been authored by UT-Battelle, LLC under Contract No. DE-AC05-00OR22725 with the U.S. Department of Energy. The United States Government retains and the publisher, by accepting the article for publication, acknowledges that the United States Government retains a non-exclusive, paid-up, irrevocable, world-wide license to publish or reproduce the published form of this manuscript, or allow others to do so, for United States Government purposes. The Department of Energy will provide public access to these results of federally sponsored research in accordance with the DOE Public Access  
20 Plan (<http://energy.gov/downloads/doe-public-access-plan>).

#### Abstract

Rapid warming of Arctic ecosystems accelerates microbial decomposition of soil organic matter and leads to increased production of carbon dioxide (CO<sub>2</sub>) and methane (CH<sub>4</sub>). CH<sub>4</sub> oxidation potentially mitigates CH<sub>4</sub> emissions from permafrost regions, but it is still highly uncertain whether soils in high-latitude ecosystems will function as a net source or sink for CH<sub>4</sub> in response to rising temperature and associated hydrological changes. We investigated CH<sub>4</sub> production and oxidation potential in permafrost-affected soils from degraded ice-wedge polygons on the Barrow Environmental Observatory, Utqiagvik (Barrow) Alaska, USA. Frozen soil cores from flat and high-centered polygons were sectioned into organic, transitional and permafrost layers, and incubated at -2, +4 and +8°C to determine potential CH<sub>4</sub> production and oxidation rates. Significant  
30 CH<sub>4</sub> production was only observed from the suboxic transition layer and permafrost of flat-centered polygon soil. These two soil sections also exhibited highest CH<sub>4</sub> oxidation potential. Organic soils from relatively dry surface layers had the lowest CH<sub>4</sub> oxidation potential compared to saturated transition layer and permafrost, contradicting to our original assumptions. Low

Deleted: polygonal

Deleted: 37831,

Deleted: 20742,

Deleted: 37831,

Deleted: 48309,

Deleted: 37831,

Deleted: to

Deleted: )

Deleted: emission

Deleted: soils. However,

Deleted: this important greenhouse gas.

Deleted: with carbon-rich soils at

Deleted: active layers, transition zones,

Deleted: Organic acids produced by fermentation fueled methanogenesis and competing iron reduction processes responsible for most anaerobic respiration.

Deleted: oxidation

Deleted: zone

Deleted: , which

Deleted: higher CH<sub>4</sub> production rates during the incubations. Although CH<sub>4</sub> production showed higher temperature sensitivity than

Deleted: potential rates of CH<sub>4</sub> oxidation exceeded methanogenesis rates at each temperature. Assuming no diffusion limitation,

methanogenesis rates are due to low overall microbial activities measured as total anaerobic respiration and competing iron reduction process. Our results suggest that CH<sub>4</sub> oxidation could offset CH<sub>4</sub> production and limit surface CH<sub>4</sub> emissions, in response to elevated temperature, and thus must be considered in model predictions of net CH<sub>4</sub> fluxes in Arctic polygonal tundra. Future changes in temperature and soil saturation conditions are likely to divert electron flow to alternative electron acceptors and significantly alter CH<sub>4</sub> production, which should also be considered in CH<sub>4</sub> models.

**Deleted:** should

## 1 Introduction

Arctic ecosystems store vast amounts of organic carbon in active layer soils and permafrost (Hugelius et al., 2014; Shiklomanov et al., 2010). Rising temperatures, increased annual thaw depth, and a prolonged thaw season accelerate microbial degradation of this carbon reservoir (Shiklomanov et al., 2010; Schuur et al., 2015; Schuur et al., 2013). The potential carbon loss due to these direct effects is estimated to be 92±17 Pg carbon over the coming century (Schuur et al., 2015). The extent of soil organic matter (SOM) decomposition and partitioning between CO<sub>2</sub> and CH<sub>4</sub> emissions highly depend upon soil saturation conditions. Thawing of ground ice and ice-wedge degradation cause ground subsidence and significant changes in soil water saturation (Liljedahl et al., 2016), generating heterogeneous surface CH<sub>4</sub> fluxes (Schädel et al., 2016), with a current estimation of the source strength ranging widely from 8 to 29 Tg C yr<sup>-1</sup> (McGuire et al., 2012). Understanding the factors that control CH<sub>4</sub> fluxes is key to reducing model uncertainties and predicting future climate feedbacks.

**Deleted:** Warmer air

**Deleted:** are increasing soil temperatures,

**Deleted:** depths

**Deleted:** length of the

**Deleted:** , exposing more of this carbon to

**Deleted:** and mineralization

**Deleted:** In addition,

**Deleted:** which could alter the future fluxes of carbon dioxide (CO<sub>2</sub>) and methane (CH<sub>4</sub>) to the atmosphere

**Deleted:** Understanding the factors that control these fluxes is key to predicting the greenhouse gas feedback on a future warming climate.

Arctic tundra acts as a large net source of CH<sub>4</sub>,

**Deleted:** The large uncertainty associated with this estimation is due to the spatial and temporal complexity of the Arctic ecosystem.

The unique polygonal ground in Arctic coastal plain tundra creates natural gradients in hydrology, snow pack depth and density, and soil organic carbon storage that control CH<sub>4</sub> fluxes (Liljedahl et al., 2016; Lara et al., 2015). Thermal contraction processes create cracks in the tundra soil, which can fill with water that freezes to produce massive ground ice (French, 2007). This ice forms wedges that create the borders of three dominant polygon types, defined by their surface relief and subsurface hydrology: low-centered polygons (LCPs), flat-centered polygons (FCPs), and high-centered polygons (HCPs) (MacKay, 2000). Poorly drained LCPs are characterized by wet centers bordered by raised, relatively dry rims and wet troughs. FCPs lack the rims of LCPs and are drier (Wainwright et al., 2015). When ice wedges erode and water drains from the polygons, troughs subside and rims disappear to form drier HCPs. Methane emissions from wet and inundated LCP sites were 1-2 orders of magnitude larger than emissions from drier FCP and HCP sites (Vaughn et al., 2016b; Sachs et al., 2010). Although a number of factors, including vegetation height and plant composition (von Fischer et al., 2010), soil inundation (Sturtevant et al., 2012), thaw depth (Sturtevant and Oechel, 2013; Grant et al., 2017), and season (Chang et al., 2014) were suggested as explanatory factors for CH<sub>4</sub> flux variations, the hundred-fold difference in CH<sub>4</sub> flux between polygon types could not be fully explained by variations in moisture or temperature (Sachs et al., 2010; Vaughn et al., 2016b). Measurements of dissolved CH<sub>4</sub> concentrations in soil pore waters suggested a huge disconnect between >100 μM concentrations of dissolved CH<sub>4</sub> in the active layer, below 20 cm and negligible dissolved CH<sub>4</sub> at 10 cm soil depth (~1 μM). δ<sup>13</sup>C-CH<sub>4</sub> data suggested CH<sub>4</sub> oxidation played

**Deleted:** about one order

**Deleted:** higher

**Deleted:** huge differences

**Deleted:** High

**Deleted:** deeper

**Deleted:** , contrasted with low

an important role in mitigating CH<sub>4</sub> in soil porewater and limiting surface CH<sub>4</sub> emissions (Vaughn et al., 2016a). However, CH<sub>4</sub> oxidation potential is rarely studied in permafrost-affected soils.

Methane oxidation mitigates terrestrial CH<sub>4</sub> emission. Up to 90% of CH<sub>4</sub> produced in the soil is consumed in the upper dry layers of soil by aerobic CH<sub>4</sub>-oxidizing bacteria (methanotrophs) before reaching the atmosphere (Le Mer and Roger, 2001). Methane oxidation rates are usually greatest in oxic, surficial soils, although methane oxidation is known to occur under oxygen-limiting conditions as well (Roslev and King, 1996). In the classical model of CH<sub>4</sub> oxidation profiles, there is usually a vertical gradient of decreasing O<sub>2</sub> concentration in the top cm of the soil column that is inversely correlated with an increasing gradient of CH<sub>4</sub> through the suboxic/anoxic active layer. The relative abundance of methanotrophs generally correlates with CH<sub>4</sub> oxidation activity at the soil surface, and methanogens are relatively abundant in the deeper layer where oxygen is limiting (Lee et al., 2015). Methane oxidation potential in wetlands and peat bogs is highest near the water table, while most CH<sub>4</sub> is produced below the water table (Whalen and Reeburgh, 2000). In contrast, methanogenic and methanotrophic communities can overlap in the rhizosphere (Liebner et al., 2012; Knoblauch et al., 2015), where roots or *Sphagnum* create an oxic/anoxic interface providing a substantial amount of oxygen for methanotrophs (Laanbroek, 2010; Parmentier et al., 2011) and organic acid substrates for methanogenesis.

Soil CH<sub>4</sub> fluxes result from the net effect of microbial CH<sub>4</sub> production and oxidation, coupled with transport processes. The rates of CH<sub>4</sub> oxidation are mainly governed by the abundance and composition of methanotrophic microbial communities and environmental factors including CH<sub>4</sub> and O<sub>2</sub> availability, soil air-filled porosity and soil-water content (Preuss et al., 2013). Previous studies of boreal lakes and wetlands showed that CH<sub>4</sub> production is more sensitive to temperature changes than CH<sub>4</sub> oxidation, as CH<sub>4</sub> oxidation rates respond more strongly to CH<sub>4</sub> availability than temperature increase (Liikanen et al., 2002; Segers, 1998). Soils at the Barrow Environmental Observatory in Utqiagvik (Barrow), Alaska experience a wide range of arctic temperatures, from -20 to +4°C (Shiklomanov et al., 2010). Soil respiration and methanogenesis continue at low temperatures close to 0 °C, even after the soil surface freezes trapping gas under ice. Therefore, substantial annual CH<sub>4</sub> and CO<sub>2</sub> emissions from the Alaskan Arctic occur during the spring thaw (Commane et al., 2017; Raz-Yaseef et al., 2017; Zona et al., 2016). However, it is unclear how accelerated warming in Arctic soils affects the opposing processes of CH<sub>4</sub> production and oxidation due to their nonlinear response to temperature changes (Treat et al., 2015).

In this study, we investigated the rates and temperature sensitivities of CH<sub>4</sub> production and oxidation from permafrost-affected soils in Utqiagvik (Barrow), Alaska. Although various studies have identified significant and frequently correlated factors affecting CH<sub>4</sub> and CO<sub>2</sub> production in permafrost ecosystems upon thawing, the oxidation of CH<sub>4</sub> is not considered in most incubation studies (Treat et al., 2015). Here we used the natural geomorphic gradient of FCP and HCP soils to represent degraded polygon tundra soils with relatively oxic active layers that will potentially act as CH<sub>4</sub> sinks. Methane production and oxidation assays were performed separately using anoxic or oxic incubations at three temperatures. We also measured

**Deleted:** from FCPs and HCPs, suggest the importance of methane oxidation in these landscape features might be underestimated .

**Moved down [1]:** 1

Soil CH<sub>4</sub> fluxes result from the net effect of microbial CH<sub>4</sub> production and oxidation, coupled with transport processes.

**Moved down [2]:** Soils at the Barrow Environmental Observatory in Utqiagvik (Barrow), Alaska experience a wide range of arctic temperatures, from -20 to +4°C (Shiklomanov et al., 2010). Soil respiration and methanogenesis continue at low temperatures close to 0 °C, even after the soil surface freezes trapping gas under ice. Therefore, substantial annual CH<sub>4</sub> and CO<sub>2</sub> emissions from the Alaskan Arctic occur during the spring thaw (Commane et al., 2017; Raz-Yaseef et al., 2017; Zona et al., 2016).

**Deleted:**

**Deleted:** However, it is unclear how rapid temperature change in Arctic soils affects the opposing processes of CH<sub>4</sub> production and oxidation due to their nonlinear response to temperature fluctuations

**Deleted:** High-affinity methanotrophs oxidize substantial amounts of atmospheric methane in high Arctic mineral soils .

**Deleted:** and

**Deleted:** immediately above

**Moved (insertion) [1]**

**Deleted:** fluctuations

**Deleted:** rapidly

**Moved (insertion) [2]**

**Field Code Changed**

**Deleted:** most

**Deleted:** sensitivity measurements for CH<sub>4</sub> processes have been performed at mesophilic temperatures that are higher than typical Arctic soil temperatures.

**Deleted:** but

**Deleted:** The coupled response of methanogenesis and CH<sub>4</sub> oxidation to increased temperature is poorly understood. Similarly, the role of fermenters that produce organic acid substrates for competing processes of methanogenesis and iron reduction is not well characterized. To improve estimates of CH<sub>4</sub> production from soils across the permafrost zone, additional research on rates of CH<sub>4</sub> oxidation is needed to scale up results from laboratory studies and to better constrain CH<sub>4</sub> budgets from permafrost region. In this study,

**Deleted:** use

**Deleted:** explore the soil organic carbon decomposition pathways and specifically test

additional mechanisms influencing CH<sub>4</sub> production, including accumulation of organic acids and competing anaerobic respiration through iron reduction. Specifically, we tested the following hypotheses regarding CH<sub>4</sub> dynamics in FCP and HCP soils: (I) CH<sub>4</sub> production is localized in the more reduced subsurface while CH<sub>4</sub> oxidation occurs at the soil surface; (II) CH<sub>4</sub> production is more sensitive to temperature increase than CH<sub>4</sub> oxidation and will likely exceed CH<sub>4</sub> oxidation in wet areas in response to warming.

## 2 Materials and Methods

### 2.1 Site description and soil sampling

The study site is located at the Barrow Environmental Observatory (BEO), Utqiagvik (Barrow), Alaska as part of the Intensive Study Site areas B (High-Centered Polygon, HCP) and C (Flat-Centered Polygon, FCP) of the Next Generation Ecosystem Experiments in the Arctic project. The centers of HCPs in area B were covered by lichens, moss and dry tundra graminoids, while centers of FCPs in area C hosted wet tundra graminoids, mosses and bare ground (Langford et al., 2016). Intact frozen soil cores from the centers of a water-saturated FCP (N 71° 16.791', W 156° 35.990') and a well-drained HCP (N 71° 16.757', W 156° 36.288') were collected with a modified SIPRE auger containing a sterilized liner, driven by a hydraulic drill during a field campaign in April 2012 (Herndon et al., 2015a; Herndon et al., 2015b; Roy Chowdhury et al., 2015). All samples were kept frozen during core retrieval, storage and shipment to Oak Ridge National Laboratory (Oak Ridge, TN). The frozen cores were stored at -20 °C until processing. The thaw depth measured in September 2012 in the HCP center was 40 cm, and thaw depths in the FCP varied from 41-47 cm.

The frozen soil cores were inspected and processed inside an anaerobic chamber (Coy Laboratories, MI. H<sub>2</sub> ≤ 2% and O<sub>2</sub> < 1 ppm). Both cores were sectioned into 10-cm segments, and each segment was inspected for evidences of roots and undecomposed organic matter. Soil Munsell color was recorded to qualitatively infer redoximorphic conditions. The soil core collected from the FCP center showed evidence of buried and discontinuous organic matter at approximately 50 cm depth, below the active, organic layer and above the permafrost. This transition layer was attributed to episodic thawing and cryoturbation (Schoor et al., 2008; Bockheim, 2007). Soil geochemical properties were measured for each 10-cm segment to assess soil geochemical depth profiles. Specifically, we measured soil gravimetric water content and soil pH, using the 1:2 soil slurry method within 1M KCl. Fe(II) concentrations were measured to characterize redox conditions in the soil segments. Briefly, a soil subsample (~2 g) was extracted with 0.1M KCl solution for 30 min in an anaerobic chamber. The extracts were filtered with 2 μm syringe filters and analyzed immediately using the colorimetric 1,10-phenanthroline method (Hach method 8146). Absorbance was determined at 510 nm using a DU 800 spectrophotometer (Beckman Coulter, CA).

**Deleted:** based on temperate ecosystem

**Deleted:** to explain CH<sub>4</sub> production

**Deleted:** organic Arctic

**Deleted:** .

**Deleted:** oxygen-depleted

**Deleted:** in

**Deleted:** layers of oxic soil.

**Deleted:** (NGEE)

**Deleted:** ORNL,

**Deleted:** depositions

**Deleted:** mineral horizon

**Deleted:** zone from 40-50 cm between active layer and permafrost

**Deleted:** No equivalent transition zone was identified in the HCP core. Both cores were sectioned into layers of 10-cm increments, and each section was inspected for evidences of roots, undecomposed organic matter, and soil Munsell color recorded to qualitatively infer redoximorphic features.

**Deleted:** .

**Deleted:** in a potassium chloride

**Deleted:** (pH<sub>KCl</sub>),

**Deleted:** concentration, total carbon and nitrogen were measured in each section as described previously, and pore water gas

**Deleted:** using the method described in Sect.

**Deleted:** 2.

## 2.2 Soil pore water gas measurements

Dissolved gas (CO<sub>2</sub> and CH<sub>4</sub>) concentrations in soil pore water were determined at each 10-cm depth-interval from the FCP and HCP cores. A 1:1 (w:v) soil slurry was prepared by mixing 10 g wet soil in 10 mL de-ionized and de-gassed water under anoxic conditions inside an anaerobic chamber. The samples were then placed in 15 mL crimp-sealed serum vials (Wheaton, NJ). Vials were inverted and shaken at 4 °C for 12 h to allow for exchange between the dissolved and soil gas phases. Then, ~5 mL of the aqueous phase was exchanged with Ar (99.9 % purity) using a Gastight syringe (Hamilton, NV), and samples were manually shaken vigorously for 5 min to allow for equilibration between the aqueous and gas phase. Subsequently, a 500-μL headspace sample was drawn and immediately analyzed with an SRI 8610C gas chromatograph using the method previously described (Roy Chowdhury et al., 2015). The detection limit for CH<sub>4</sub> was 1 ppmv. Concentrations of CH<sub>4</sub> and CO<sub>2</sub> were corrected for dissolved gases based upon temperature and pH-dependent Henry's Law constants (Sander, 2015).

## 2.3 Low temperature respiration experiments

To investigate the temperature response of CH<sub>4</sub> production and overall organic carbon mineralization rates, samples of FCP and HCP soil cores were incubated at -2, +4 or +8 °C for approximately 90 days. Based on measured geochemical similarities, core segments were combined to represent the organic layer that comprises most of the active layer, transition layer (only present in FCP), and permafrost. Soils from each layer were homogenized inside an anaerobic chamber using sterile tools and equipment to establish microcosms. Gas mixtures for the microcosm headspaces were selected based on gravimetric water contents and concentrations of reduced Fe(II) (Howeler and Bouldin, 1971) to best represent field conditions. Thus, organic layer soils from both FCP and HCP cores were incubated under air, while the transition layer and permafrost of FCP and HCP cores were incubated under anoxic conditions with N<sub>2</sub> headspaces. Anoxic microcosms were flushed with N<sub>2</sub> three times after sealing to remove residual H<sub>2</sub> and O<sub>2</sub> from the headspace. It is important to note that at -2 °C soil water remained unfrozen in these samples due to freezing point depression (Romanovsky and Osterkamp, 2000).

A subsample of the combined, homogenized soil (~10 g) was placed in a sterile 70-mL serum bottle sealed with a blue butyl stopper and aluminum crimp seal to form a soil microcosm. For each homogenized soil layer, 9 replicate microcosms were constructed at each incubation temperature (Figure 1). Headspace CO<sub>2</sub> and CH<sub>4</sub> concentrations were measured at 2 to 15 days' intervals using gas chromatography (see Section 2.2). After 5, 10 or 20 days of incubation, three replicated microcosms were destructively sampled for methane oxidation assays (see section 2.4 and Figure 1) and additional soil geochemical analysis.

Subsamples from microcosms opened after 10, 20 and 90 days' incubation were further processed for analysis of pH, Fe(II) and total organic acids. pH and Fe(II) concentrations were measured as described in section 2.1. Iron reduction rates were estimated by the changes in measured Fe(II) concentration. Organic acids were analyzed using NH<sub>4</sub>HCO<sub>3</sub> extracts. Briefly, NH<sub>4</sub>HCO<sub>3</sub> extractions (12 h) were centrifuged for 15 min at 6500 g, then the supernatants were filtered through 0.2-μm

**Deleted:** ¶

Based on similarities in the above mentioned geochemical properties, several soil sections were combined to represent the active layer, transition zone and upper permafrost. The top 10 cm of the cores contained substantial ice or plant material; these sections were not used for soil incubation studies. The next two sections (comprising 10-30 cm depth) were combined to represent the active layer, for both FCP and HCP cores. The FCP section from 40-50 cm depth provided transition zone samples. Finally, sections from 50-70 cm depth were combined to represent permafrost layer soils for both cores. Soils from each layer were homogenized inside the anaerobic chamber using sterile tools and equipment. The homogenized soil from each layer was sub-sampled for microcosm incubation studies described below. ¶

**Deleted:** 2.3 Soil microcosm setup, methane oxidation potential assay and soil chemical analyses ¶  
**2.3.1 Temperature sensitivity of CO<sub>2</sub> and CH<sub>4</sub> production from unamended microcosms ¶**

**Deleted:** (measured as CO<sub>2</sub> production), homogenized soils described in section 2.1 from the

**Deleted:** or

**Deleted:** zone

**Deleted:** were used in incubations (Table S1). Replicate (n=9) microcosms of each homogenized soil layer were constructed in sterile 70 mL serum bottles sealed with blue butyl stoppers and aluminum crimps.

**Deleted:** FCP

**Deleted:** HCP core layers were incubated under anoxic or oxic conditions, determined by the

**Deleted:** measured in each layer

**Deleted:** . Microcosms

**Deleted:** active layers of

**Deleted:** prepared in oxic conditions with ambient laboratory

**Deleted:** . Microcosms from

**Deleted:** zone

**Deleted:** the permafrost layer of HCP were set up inside the anaerobic chamber.

**Deleted:** All microcosms contained ~10 g wet soil, and they were incubated at -2, +4 or +8 °C for approximately 90 days.

**Deleted:** 2.3.2

membrane filters before analysis. Filtered sample were analyzed for low-molecular-weight organic acids using a Dionex ICS-5000<sup>+</sup> system (Thermo Fisher Scientific, MA) equipped with an IonPac AS11-HC column with a KOH mobile phase. Total organic acid concentrations ( $T_{OA}$ ) were calculated by summing molar C equivalents for each measured species, normalized per gram of dry soil.

Moved (insertion) [3]

#### 2.4 Methane oxidation potential assay

Soil samples were incubated in oxic conditions supplemented with ample  $CH_4$  substrate to measure  $CH_4$  oxidation potential (Roy Chowdhury et al., 2014). Methanogenesis is expected to be negligible under these oxic conditions. The methane oxidation assays (MOAs) were constructed using both freshly thawed (labeled as 0 day) and pre-incubated (labeled as various days of pre-incubation) samples to account for potential delays in the overall microbial activities (Figure 1). Replicated samples (about 2 g) were slurried in a 1:1 (w:v) ratio with autoclaved de-ionized water in 26 mL serum bottles under ambient condition. A 1%  $CH_4$  headspace was introduced into each crimp-sealed bottle by replacing 0.23 mL headspace with 99.99%  $CH_4$  (Scott, Air Liquide). For freshly thawed samples, 9 replicates were constructed for each incubation temperature and each soil layer. For pre-incubated samples at the designated sampling day, 3 replicated incubations (~10 g per sample) were destructively sampled to construct 9 replicates of MOAs to incubate at the same incubation temperature they were pre-incubated (Figure 1). Due to the limited number of shaking-incubators, only the 4 °C MOA from FCP and 8 °C MOA from HCP were shaken to minimize potential gas-liquid phase transfer limitations. Headspace  $CO_2$  and  $CH_4$  concentrations in MOAs were measured at 2 to 15 days' time intervals using gas chromatography (section 2.2).

Moved (insertion) [4]

Deleted: After 0, 10 or 20 days of microcosm incubation described in section 2.3.1, three replicates corresponding

Deleted: each layer and temperature were opened to set up  $CH_4$

Deleted: and further analyses. Replicate (n=9)

Deleted: from each time point

Deleted:

Deleted: oxic conditions.

Deleted: . Samples

Deleted: as the microcosms from which

Deleted: harvested. To eliminate

Deleted: limitation, samples from FCP were shaken and incubated at 4 °C, and samples from HCP were shaken and incubated at 8 °C.

Deleted: soil incubations and methane oxidation assays

Deleted: as described in

Deleted:

Deleted: 3.3 Extractable ion analysis<sup>¶</sup>

Deleted: Aliquots of soil samples from microcosms opened after 10, 20 and 90 days of incubation were extracted with either 10 mM  $NH_4HCO_3$  (pH ~ 7.3) or 0.1 M KCl (pH~

Deleted: 0) solution for determining soil organic acids and extractable Fe(II), respectively. Briefly,  $NH_4HCO_3$  extractions (12 h) were centrifuged for 15 min at 6500 g, and the supernatants were further filtered through 0.2  $\mu$ m membrane filters before analysis.

Moved up [3]: Filtered sample were analyzed for low-molecular-weight organic acids using a Dionex ICS-5000<sup>+</sup> system (Thermo Fisher Scientific, MA) equipped with an IonPac AS11-HC column with a KOH mobile phase.

Deleted: Fe(II) concentrations from filtered KCl extract samples were diluted and quantified using the HACH Ferrous method 8146 (1,10-phenanthroline). Absorbance was measured at 510 nm using a DU 800 spectrophotometer (Beckman Coulter, CA). Soil pH was determined using the slurry method by mixing a 1:5, w:v ratio of soil to 1M KCl.

Moved up [4]: ¶  
2.4

Deleted: accumulated over time in

Deleted: S1. To estimate temperature sensitivity, gas production rates at -2, +4, and +8 °C were fit to the exponential Arrhenius equation, and a quotient of rates ( $Q_{10}$ ) is calculated as described previously.

Deleted: mass basis

Deleted: active

Deleted: zone

#### 2.5 Rate estimation, temperature sensitivity and statistical analyses

Concentrations of  $CH_4$  and  $CO_2$  from soil microcosms were fitted with hyperbolic, sigmoidal, or linear functions (Roy Chowdhury et al., 2015). Rates of  $CO_2$  production were calculated using derivatives of the best curve-fitting equations with parameters listed in Table S3. Methane oxidation rates were calculated from the loss of headspace  $CH_4$ , which were best fitted with simple linear regression. All rate calculations are reported on per gram soil dry weight basis. The temperature dependence was calculated using the conventional  $Q_{10}$  relationship by taking the ratio of maximum production or oxidation rates at 8 and -2 °C based on triplicate measurements.

Changes of soil physicochemical properties were evaluated with one-way ANOVA, Tukey's Honest Significant Difference (HSD) test. The effect of soil layers (organic, transition layer, and permafrost) and incubation temperature (-2, 4 and 8 °C) were examined with Tukey's HSD test. All curve fittings and statistical analyses are performed with R 3.4.0 (The R Foundation for Statistical Computing) and validated with Prism (GraphPad Software, ver. 7.0a).

## 2.6 Calculation of net CH<sub>4</sub> emission

To evaluate the net result of CH<sub>4</sub> production and oxidation and how this result changes in response to temperature increase, we applied a simplified model simulation. Representation of the CH<sub>4</sub> oxidation rate ( $R_{oxi}$ ) is based on Michaelis-Menten kinetics with linear dependence on the biomass of methanotrophs (Xu et al., 2015), while the CH<sub>4</sub> production rate ( $R_{pro}$ ) is calculated from measurements directly.

$$R_{oxi} = B_{methanotrophs} \cdot V_{max,oxi} \left[ \frac{C_{CH_4}}{C_{CH_4} + K_{m,CH_4}} \right] \left[ \frac{C_{O_2}}{C_{O_2} + K_{m,O_2}} \right]$$
$$R_{pro} = B_{methanogens} \cdot V_{measure,pro}$$

where  $B_{methanotrophs}$  and  $B_{methanogens}$  represent the estimated biomass of methanotrophs and methanogens respectively.  $K_{m,CH_4}$  and  $K_{m,O_2}$  are the half saturation coefficients (mM) with respect to CH<sub>4</sub> and O<sub>2</sub> concentrations, respectively. Values of  $K_{m,CH_4}$  and  $K_{m,O_2}$  vary within different models. We started with  $K_{m,CH_4} = 0.005$  and  $K_{m,O_2} = 0.02$  (Riley et al., 2011) and further applied a wide uncertainty range of 0.0005-0.05, 0.002-0.2. The maximum CH<sub>4</sub> oxidation rate  $V_{max,oxi}$  and CH<sub>4</sub> production rate  $V_{measure,pro}$  were obtained from the incubations. Initial CH<sub>4</sub> and O<sub>2</sub> concentrations were calculated from soil porewater dissolved gas measurement and soil air-filled porosity estimations. With the above parameters, we estimated the biomass ratio of methanogens to methanotrophs ( $B_{methanogens} / B_{methanotrophs}$ ) under both net CH<sub>4</sub> production and net CH<sub>4</sub> oxidation scenarios, and further evaluated how the biomass ratio would change in response to rising temperature to keep the soil as a net source or sink of CH<sub>4</sub>.

## 3 Results

### 3.1 Soil attributes and pore water characteristics

Soil cores from FCP and HCP center positions showed distinct vertical profiles of soil moisture expressed as gravimetric water content (g g<sup>-1</sup> dry soil). The soil core from FCP was characterized by a wet surface within the top 10 cm below ground, a much drier organic layer between 10 to 40 cm, and a bottom layer below 40 cm with significantly higher water content. In the HCP core, soil moisture gradually increased from the top to the bottom (Figure 2). Soil bulk density (g cm<sup>-3</sup>) is negatively correlated with gravimetric water content in both FCP and HCP along the depth profile ( $R^2 = -0.93$ , and  $R^2 = -0.86$ , respectively). A similar water distribution has been recorded by continuous field measurements of volumetric water content at the nearby NGEE\_BRW\_C soil pit monitoring site (<http://permafrostwatch.org>). Fe(II) concentration showed a strong positive correlation with gravimetric water content in both FCP and HCP cores ( $R^2 = 0.81$ , and  $R^2 = 0.91$ , respectively). The soil pH in FCP increased steadily with soil depth ( $R^2 = 0.95$ ), with an average of 4.7. In the HCP soil core, soil pH varied by 1.5 pH unit, with an average of 5.4. Overall, soil moisture, Fe(II) concentration and pH increased with depth in the centers of both polygon types.

Deleted: 5

Deleted: a

Deleted: in Eq. (1)

Deleted: using Eq. (2).

Deleted: (1)

Deleted: (2)

Deleted: are 0.005 and 0.02, with ranges of 0.0005-0.05, 0.002-0.2, respectively

Deleted: .

Deleted: By assuming  $R_{oxi} = R_{pro}$ , the ratio of  $B_{methanogens}$  to  $B_{methanotrophs}$  can be calculated at different temperatures.

Deleted: intermediate

Deleted: (Fig. 1)

Deleted: Soil moisture from the HCP core gradually increased from the top to the bottom (Fig. 1), consistent with field measurements of the water level in nearby HCPs .

Deleted: of HCP

Dissolved CO<sub>2</sub> in soil pore water showed a similar general trend in both FCP and HCP cores. The concentration of dissolved CO<sub>2</sub> increased from 100 μM in the surface soil (0-10 cm) to approximately 950 μM at 30 to 40 cm depth in FCP, and it decreased below 40 cm. In HCP, approximately 400 μM dissolved CO<sub>2</sub> was measured in the surface soil. The concentration was 400-500 μM in the top 30 cm and also decreased significantly below 40 cm. A strong correlation between dissolved CO<sub>2</sub> concentration and soil bulk density was observed for both FCP and HCP ( $R^2=0.91$ , and  $R^2=0.85$ , respectively).

**Deleted:** was between 0.2 to 0.6 μmol g<sup>-1</sup> dry soil

**Deleted:** first

**Deleted:** 0.9 to 1.6 μmol g<sup>-1</sup> dry soil

**Deleted:** 50 cm.

The highest dissolved CH<sub>4</sub> concentration (about 85 μM) was found between 30 to 40 cm in soil pore water of FCP, approximately 10 times the CH<sub>4</sub> concentration measured from the top 10 cm and 2-4 times higher than the CH<sub>4</sub> concentration measured below 40 cm. In HCP, significant CH<sub>4</sub> accumulation in soil pore water was found below 50 cm of the HCP core, while no dissolved CH<sub>4</sub> was detected above 50 cm.

**Deleted:** 40

**Deleted:** 50

**Deleted:** 4

**Deleted:** (Fig. 1).

**Deleted:** The active

Soil cores of FCP and HCP were divided into organic, transitional and permafrost layers to facilitate incubation setup. The top 10 cm of both cores contained mostly plant material, litter and ice or snow: these sections contained little soil and were not studied further. The organic layers of FCP and HCP cores were both oxic, with low Fe(II) concentrations and minimal dissolved CH<sub>4</sub> in soil pore water, while deeper layers were more reduced, with 5-7 fold higher Fe(II) concentrations and more dissolved CH<sub>4</sub> (Figures 1 and S1). Measured total carbon and nitrogen content showed distinct patterns in FCP and HCP cores (Table S1). The total carbon content of the FCP permafrost (31%) was nearly twice as large as the organic layer. The FCP transition layer contained much less carbon than the adjacent layers (20% of FCP permafrost), leading to a low C/N ratio of 16. For the HCP, the total carbon contents of organic and permafrost layers were 21% and 17%, respectively, significantly lower than that of the FCP permafrost. Inorganic carbon quantified as CO<sub>2</sub> released upon acid treatment was less than 0.001% for each layer of the FCP and HCP cores.

**Deleted:** and suboxic with significantly higher Fe(II) concentrations and dissolved CH<sub>4</sub> (Fig. S1).

### 3.2 Temperature responses of CH<sub>4</sub> production and oxidation

Thawed FCP and HCP soil samples were incubated in microcosms at fixed temperatures to assess methanogenesis rates. CH<sub>4</sub> production was only observed in microcosms from the transition layer and permafrost of FCP, which were incubated under anoxic conditions. CH<sub>4</sub> production started within 5 days after the anoxic incubations were set up (Figure 3). Cumulative CH<sub>4</sub> concentrations at all temperatures were best fitted with a linear model (Table S2). Soils from the transition layer yielded about 10 times more CH<sub>4</sub> than permafrost at same incubation temperatures. Transition layer soil showed a stronger temperature effect than permafrost. CH<sub>4</sub> production rate increased by 1.6 and 3.1 times as the temperature increased from -2 °C to 4 °C and 8 °C, respectively. Measurements of CH<sub>4</sub> concentrations in the headspace of HCP permafrost were mostly below the quantification limit of the gas chromatograph flame ionization detector (1ppmv, Figure S2). Organic soils from both FCP and HCP were

**Deleted:** The total carbon content of the FCP permafrost (31%) was nearly 66% greater than the active layer content and five-fold more than the transition zone (Table S1). The total carbon content of active and permafrost layers of HCP were 21% and 17%, respectively, and substantially lower than that of the FCP permafrost. Inorganic carbon quantified as CO<sub>2</sub> released upon acid treatment was less than 0.001% for all layers of the FCP and HCP cores.

#### 3.2 CH<sub>4</sub> production and oxidation rates 3.2.1 CH<sub>4</sub> production

**Deleted:** To emulate the natural redox gradient, FCP and HCP active layer samples were incubated in oxic conditions, while transition zone and permafrost samples were incubated in anoxic conditions, as described in Sect. 2.3.1.

**Deleted:** zone

**Deleted:** was detected

**Deleted:** Fig. 2

**Deleted:** Samples from the transition zone yielded about 10 times more CH<sub>4</sub> than permafrost layer samples.

incubated with air to best represent the field condition, and methanogenesis was unlikely to occur under oxic conditions. Headspace O<sub>2</sub> was not completely consumed after 90 days incubation (calculations not shown).

Potential rates of aerobic CH<sub>4</sub> oxidation were measured in freshly thawed and pre-incubated soils to minimize total microbial growth limitations. Pre-incubated soils showed much higher CH<sub>4</sub> oxidation potential compared to corresponding freshly thawed soil in both FCP and HCP. In FCP soil, CH<sub>4</sub> oxidation potentials measured in soils from the transition layer and permafrost were significantly higher than those measured in organic soils (Figure 4a, 4b). Similarly, permafrost from HCP showed higher CH<sub>4</sub> oxidation potentials than organic soils (Figure 4c, 4d). Overall, CH<sub>4</sub> oxidation rates in HCP soils were 80-90% lower than rates from the equivalent FCP soil layers.

Rates of both CH<sub>4</sub> production and oxidation responded positively to temperature increase (Figure 5). In the transition layer of FCP, CH<sub>4</sub> production showed much higher temperature sensitivity than CH<sub>4</sub> oxidation from both freshly thawed and pre-incubated soils, with an estimated Q<sub>10</sub> value of 4.1. The Q<sub>10</sub> value of CH<sub>4</sub> oxidation was 2.0 from freshly thawed soils and only 1.1 in pre-incubated soils. Similarly, the Q<sub>10</sub> value for CH<sub>4</sub> oxidation in permafrost also dropped from 1.7 in freshly thawed soils to 1.0 in pre-incubated soils. However, CH<sub>4</sub> production in the permafrost responded slowly to temperature increase, with an estimated Q<sub>10</sub> value of 1.7. Overall, permafrost showed significantly lower CH<sub>4</sub> production rates than soils from the upper transition layer, and also had a much lower temperature sensitivity for CH<sub>4</sub> production. However, the measured CH<sub>4</sub> oxidation potentials were similar in both soils, with similar temperature responses.

### 3.4 Soil respiration in response to rising temperature

Total soil respiration was evaluated using CO<sub>2</sub> production to characterize the observed variation in CH<sub>4</sub> production. Soils in all of the microcosm incubations produced CO<sub>2</sub>, by aerobic respiration under oxic conditions or by anaerobic respiration and fermentation under anoxic conditions. CO<sub>2</sub> production started immediately in microcosms of FCP samples, including organic soils that were incubated under oxic conditions and soils from transition layer and permafrost samples that were incubated under anoxic conditions (Figure 6). CO<sub>2</sub> accumulation was best modeled by a hyperbolic function, except the organic layer soil incubated at -2 or +4 °C where the best fit was a linear function (Table S3, Figure 6). This exception is likely due to continuous aerobic respiration at lower temperatures, indicating that substrate limitation was not reached within 90 days. The transitional layer had the slowest CO<sub>2</sub> production rates and least carbon loss via CO<sub>2</sub>, in contrast to its relatively high rate of methanogenesis.

CO<sub>2</sub> production in microcosms of HCP samples was significantly delayed with much lower production compared to FCP soils. The HCP cumulative CO<sub>2</sub> production profiles were best fitted with a sigmoidal model, compared to the hyperbolic model that best fit FCP data (Table S3). A prolonged delay in CO<sub>2</sub> accumulation was observed in both HCP organic and permafrost

**Deleted:** CH<sub>4</sub> concentrations measured from both HCP layers, and the active layer of FCP were all below the detection limit of 1 ppm, (Fig. S2). Methanogenesis was unlikely to occur in the active layers from FCP and HCP as these microcosms were incubated under oxic conditions, and our calculation suggested that O<sub>2</sub> was not completely consumed after 90 days incubation (data not shown).

#### 3.2.2 Methane oxidation potential

**Deleted:** as described in Sect. 2.3.2 using

**Deleted:** (0 day and 5 days) and soils that had been previously incubated (10 days and 20 days pre-incubation) in the microcosms described in Sect. 2.3.1. Potential

**Deleted:** (Fig. 3). CH<sub>4</sub> oxidation potentials from transition zone and permafrost soils were more than twofold higher than the active layer in freshly thawed FCP samples (Fig. 3a). Similar to FCP soils, freshly thawed HCP permafrost showed slightly higher CH<sub>4</sub> oxidation potentials than active layer soil (Fig. 3c).

**Deleted:** Pre-incubated soils from FCP microcosms showed similar CH<sub>4</sub> oxidation potentials to newly thawed soils at +8 °C (Fig. 3). However, the potential increased significantly in transition zone samples incubated at -2 °C ( $p=0.01$ ), perhaps due to methanotroph biomass increasing in response to methanogenesis during the 20 day pre-incubation. HCP permafrost layer samples obtained after 10 days of anoxic incubation also show higher CH<sub>4</sub> oxidation potentials ( $p<0.05$ , Fig. 3c, 3d).

#### 3.3 Temperature sensitivity of CH<sub>4</sub> production and oxidation

Potential CH<sub>4</sub> production rates from both transition zone and permafrost of FCP were significantly higher at +8 °C than -2 °C ( $p < 0.01$ , t-test). Transition zone soil showed a stronger temperature response, with a Q<sub>10</sub> value of  $4.2 \pm 0.9$ , compared to  $1.7 \pm 0.7$  for permafrost.

The temperature dependency of CH<sub>4</sub> oxidation was consistent among soils layers. CH<sub>4</sub> oxidation potentials significantly increased when the incubation temperature increased from -2 to +8 °C in active

**Deleted: and its temperature sensitivity**

**Deleted:** (day 1)

**Deleted:** (Fig. 4). Soils from the active layer

**Deleted:** initial

**Deleted:** .

**Deleted:** these oxic soils produced 10 times more CO<sub>2</sub> after prolonged incubations compared to

**Deleted:** zone

**Deleted:** .

**Deleted:** modelled

**Deleted:** active

**Deleted:** Fig. 4

**Deleted:** transition zone

**Deleted:** CO<sub>2</sub> production in microcosms of HCP samples showed a different pattern from FCP samples. For active layer soils, the... [2]

**Deleted:** active

samples. CO<sub>2</sub> production started about 10 days after the microcosm setup in the organic layer and reached a maximum rate at 30 days (+4 and +8 °C) or 75 days (-2 °C). The delay was longer in permafrost incubations, with a rapid increase after 40 to 50 days followed by a plateau. Therefore, microorganisms mineralized more carbon from FCP soils than HCP soils, and CO<sub>2</sub> production began sooner in FCP than HCP soil incubations.

Deleted: layer

Deleted: active

Temperature showed significant effects on CO<sub>2</sub> production from the organic and transitional layers of FCP during 90-day incubations ( $p < 0.01$  for each layer, Figure 6). FCP soils incubated at +8 °C produced substantially more CO<sub>2</sub> than those incubated at lower temperatures. In the permafrost layer of FCP, CO<sub>2</sub> production was significantly higher at +8 °C compared to 2 °C ( $p < 0.05$ , ANOVA with Tukey's multiple comparisons test). Anaerobic CO<sub>2</sub> production in FCP permafrost showed much higher temperature sensitivity than that from FCP transition layer ( $Q_{10} = 2.3-3.3$  and  $1.2-1.3$ , respectively, Table S4).

Deleted: active layer

Deleted: transition zone

Deleted:

Deleted: ) (Fig. 4

Deleted: The temperature sensitivity for CO<sub>2</sub> production in FCP soils was highest for oxic active layer FCP samples ( $Q_{10} = 5.8 \pm 1.8$ ) and lower for anoxic transition zone and permafrost samples ( $Q_{10} = 0.9 \pm 0.6$  and  $2.2 \pm 1.0$ , respectively estimated for day 1). The  $Q_{10}$  values of HCP active and permafrost layers could not be readily estimated from sigmoidal models due to different lag periods, but were empirically estimated at  $2.7 \pm 0.02$  and  $2.6 \pm 1$ , respectively. Therefore, the FCP active layer aerobic mineralization was most sensitive to a temperature rise, while the anaerobic processes in the transition zone and permafrost had a temperature sensitivity typical of many soils (discussed below).

Deleted: transition zone

Deleted: I

Deleted: most abundant

Deleted: Concentrations of dominant organic acids measured in the permafrost were approximately 10 times higher than those measured in the transition zone. The difference was associated with lower total carbon content (5.8%) in the transition zone than that in the permafrost (30.8%). Significant increases in acetate concentration after the incubation were observed from both transition zone ( $p = 0.02$ ) and permafrost ( $p = 0.02$ ) layers, while formate and propionate decreased by up to 40% in both layers.

Incubation temperature showed a profound impact on the acetate dynamics. In the transition zone, acetate concentration increased by 56%, 142%, and 156% at -2, 4, and 8 °C, respectively after the incubation. Acetate concentrations in permafrost samples increased from high initial values by 17%, 39% and 53%, respectively.

### 3.5 Organic acids production and iron reduction in FCP soils

Organic acids were produced as intermediate metabolites during microbial degradation of organic matter, and they probably fueled methanogenesis and iron reduction. Specific organic acids were analyzed from soil extracts from FCP transitional and permafrost layers (Table S5). The dominant organic acids included formate, acetate, propionate, butyrate, and oxalate, consistent with previous analyses from LCP soils (Herndon et al., 2015a). Trace amount of lactate, pyruvate, and succinate were detected, with concentrations less than 0.05  $\mu\text{mol g}^{-1}$  soil. To compare the changes in organic acids over time, total organic carbon contained in formate, acetate, propionate, butyrate and oxalate products was calculated ( $T_{OA}$ ,  $\mu\text{mol C g}^{-1}$ , Figure 7a,b). Concentrations of dominant organic acids measured in the permafrost were approximately 10 times higher than those measured in the transition layer. The difference could be partly explained by much lower SOC content (5.8%) in the transitional layer than that in the permafrost (30.8%).  $T_{OA}$  increased by 23%, 70% and 65% at -2, 4 and 8 °C, respectively, in transitional soils during 90-day anoxic incubations. Permafrost initially contained a much higher concentration of organic acids, and  $T_{OA}$  increased by a lower percentage, by 1%, 15% and 25% at -2, 4 and 8 °C, respectively.

Deleted: ), and the changes during the incubation were plotted for each layer of FCP (Fig. 5).  $T_{OA}$  drastically dropped to near zero in the active layer due to the aerobic decomposition. Under anaerobic conditions,  $T_{OA}$  generally increased during the incubations, except for permafrost incubated at 4 °C.

Deleted: changes

Deleted: Fig. 6

Deleted: zone

Deleted: initial levels

Deleted: zone

Deleted: transition zone

Deleted: transition zone

Deleted: , respectively

Significant increases in Fe(II) concentrations were observed from anoxic incubations of FCP samples over the incubation period (Figure 7c,d). In soils from the transition layer, Fe(II) concentrations stayed at a similar level during the first 20 days of anoxic incubation, and then increased significantly from  $\sim 50 \mu\text{mol g}^{-1}$  to  $\sim 100 \mu\text{mol g}^{-1}$  during the 20 to 90 days incubation period at -2, 4 and 8 °C. In the permafrost, the highest level of iron reduction within the first 20 days was observed in samples incubated at -2 °C. Between 20 and 90 days, the highest iron reduction rates were observed in samples incubated at 8 °C. The estimated  $Q_{10}$  values were 1.2 and 1.3 for transition layer and permafrost, respectively. If we assume that iron reduction is coupled to acetate oxidation to produce CO<sub>2</sub>, stoichiometric calculations suggest that iron reduction could account for 96% and 70% of CO<sub>2</sub> produced in the transitional and permafrost layers at -2 °C. At 8 °C iron reduction could account for 74% and 61% of acetate oxidation in the transitional and permafrost layers.

#### 4 Discussion

The widespread ice-wedge degradation in the Arctic causes morphological succession and hydrological changes in tundra ecosystems (Liljedahl et al., 2016). FCP and HCP features represent successively more degraded polygons. Despite clear

5 geomorphological differences between polygon types that affect drainage, vegetation and snow cover, the frozen FCP and HCP organic layers share similar gravimetric water contents, pH, SOC, and Fe(II) concentrations. Permafrost from both polygons contains more water, dissolved CH<sub>4</sub>, and Fe(II) than organic layer soils indicating more reducing environments. Concentrations of CH<sub>4</sub> measured in soil pore water from FCP and HCP cores increased with depth. These results are consistent with field measurements of CH<sub>4</sub> dissolved in soil water sampled from the sites during the thaw season (Herndon et al., 2015b).

10 This CH<sub>4</sub> gradient suggests CH<sub>4</sub> oxidation in the upper organic layer. Therefore, we developed the following hypotheses for CH<sub>4</sub> production and oxidation, which were informed by previous studies of methane cycling in temperate ecosystems but untested in the Arctic. (1) CH<sub>4</sub> is produced in the more reduced subsurface, and consumed by methane oxidizers at the upper section of the soil column where O<sub>2</sub> is available. (2) Methane production has higher temperature sensitivity than CH<sub>4</sub> oxidation, and is likely to exceed the CH<sub>4</sub> consumption rate in wet areas in response warmer temperature.

15 Aerobic CH<sub>4</sub> oxidation is usually assumed to be limited by O<sub>2</sub> and CH<sub>4</sub> diffusion. Therefore, upper layers of soil, the rhizosphere and soil at the water table would be expected to have the highest CH<sub>4</sub> oxidation activities (Shukla et al., 2013; Gullledge et al., 1997). The abundance of the *pmoA* marker gene for CH<sub>4</sub> oxidation decreased with soil depth in HCP trough soils (Yang et al., 2017) and in permafrost-affected soils from the Canadian Arctic (Frank-Fahle et al., 2014), consistent with

20 that conceptual model. Thus, the organic layers of FCP and HCP in the BEO tundra would have higher potential for CH<sub>4</sub> oxidation. However, the highest CH<sub>4</sub> oxidation potentials were measured in the transitional and permafrost layers of FCP, the only layers with active methanogenesis. This result suggests that most active methanotrophs are found in these deeper soil layers.

25 Our results demonstrated CH<sub>4</sub> oxidation might not be primarily O<sub>2</sub> diffusion-limited, but rather limited by the availability of CH<sub>4</sub> in this system. The highest CH<sub>4</sub> oxidation potentials were measured below the rhizosphere, in suboxic layers where CH<sub>4</sub> has accumulated. Given that half-saturation constants for CH<sub>4</sub> and O<sub>2</sub> used in methanotrophy models vary over 1-2 orders of magnitude (Segers, 1998; Riley et al., 2011), aerobic CH<sub>4</sub> oxidation could occur throughout much of the soil column, as advective, diffusive or plant-mediated transport processes introduce O<sub>2</sub> into the soil. Others have observed deep soil CH<sub>4</sub>

30 oxidation activity in peatlands (Hornibrook et al., 2009), fens (Cheema et al., 2015) and wet tundra (Barbier et al., 2012), often correlated with water table depth (Sundh et al., 1994).

Deleted: active

Deleted: were

Deleted: in terms of their

Deleted: active

Deleted: CH<sub>4</sub>

Deleted: pore

Deleted: using piezometers

Deleted: The disconnect between

Deleted: trapped in the permafrost layer and trace amounts of dissolved CH<sub>4</sub> in active layer samples

Deleted: active

Deleted: began this work with

Deleted: near-surface

Deleted: and

Deleted: activity

Deleted: relative

Deleted: we would expect that

Deleted: active

Deleted: the highest rates of

Deleted: transition zone

Deleted: .

The water table in the center of Barrow LCPs and FCPs varies somewhat during the thaw season but remains close to the surface (<10 cm below surface for most of the thaw season) (Liljedahl et al., 2015; Liljedahl et al., 2016). Precipitation balances evapotranspiration during the thaw season, with little lateral runoff (Dingman et al., 1980), and volumetric water contents remain constant for these features (<http://permafrostwatch.org>). In HCPs, the water table drops up to 20 cm below the surface following snowmelt (Liljedahl et al., 2015), and the soils have a lower volumetric water content. Due to limited drainage in the flat coastal plain, the frozen cores analyzed here are representative of field conditions for much of the thaw season. Water isotope analysis demonstrated that most water in the deep active layer comes from summer precipitation rather than seasonal ice melt (Throckmorton et al., 2016). Precipitation during September and October 2011 was above average for Barrow (<http://climate.gi.alaska.edu/>), suggesting a high water table and limited gas diffusion during the winter freeze-up before we collected soil cores in early 2012. As a result of these annual and transient changes in saturation, methanotrophs could colonize a broad range of the soil column below the rhizosphere. A comparison of methanogenesis and methane oxidation potential in peat bogs demonstrated that methanotrophs survived temporary exposure to anoxic conditions, suggesting these organisms can tolerate rapid changes in the water table and redox potential (Whalen and Reeburgh, 2000). These observations argue against hypotheses that CH<sub>4</sub> oxidation occurs primarily at the surface layer or at the water table interface.

The net effect of CH<sub>4</sub> production and oxidation, in response to temperature change determines the sign of surface-atmosphere CH<sub>4</sub> flux. The 4.1-fold increase in CH<sub>4</sub> production in the transition layer due to a 10 °C rise in temperature (Q<sub>10</sub>) was similar to the average value of 4.26 reported in a recent meta-analysis of permafrost-affected soils (Schädel et al., 2016). These values are substantially higher than the temperature sensitivity of CH<sub>4</sub> oxidation from both freshly thawed and pre-incubated samples (Q<sub>10</sub> = 1 to 2). While both CH<sub>4</sub> production and oxidation respond positively to increased temperature, CH<sub>4</sub> production rates are predicted to increase more rapidly with higher temperature at this critical interface between the organic layer and permafrost. This difference in temperature sensitivity of CH<sub>4</sub> production and oxidation was also found in Arctic lakes (Lofton et al., 2014). CH<sub>4</sub> oxidation potential from freshly thawed FCP soils showed a temperature sensitivity coefficient (Q<sub>10</sub>) between 1.7 and 2.0, which is consistent with reported values from peat (Segers, 1998). Higher Q<sub>10</sub> values for CH<sub>4</sub> oxidation were reported in drier mineral Arctic cryosols with low organic carbon content (Jørgensen et al., 2015; Christiansen et al., 2015).

Assuming no diffusion limitation, we evaluated the net effect of CH<sub>4</sub> production and oxidation based on rate measurements from the transitional layer of FCP that exhibited the highest CH<sub>4</sub> oxidation potential. Methane oxidation rates are 14, 9, and 7 times the methanogenesis rate at -2, 4, and 8°C, respectively. It is quite likely that methanogenesis will outpace CH<sub>4</sub> oxidation under much warmer temperature if there is no change in soil water content. We introduced model representations to explore this possibility, as previous studies suggest CH<sub>4</sub> oxidation rate is strongly regulated by the CH<sub>4</sub> supply (Liikanen et al., 2002; Lofton et al., 2014). Without diffusion limitations, we modeled the distribution of the active biomass ratio between methanogens and methanotrophs ( $B_{\text{methanotrophe}}/B_{\text{methanogens}}$ ), which would cause Arctic soils to act as CH<sub>4</sub> sink or source in response to rising temperature (Figure 8). Given the large difference in the rates of CH<sub>4</sub> production and oxidation, CH<sub>4</sub>

**Deleted:** Cold water from precipitation mixing

**Deleted:** could provide methanotrophs with sufficient oxygen to grow

**Deleted:** , close to the methane source

**Deleted:** the hypothesis

**Deleted:** Temperature disparately affects

**Deleted:** , leading to a complex

**Deleted:** in net

**Deleted:** 2

**Deleted:** zone

**Deleted:** 0

**Deleted:** active

**Deleted:** When methanotrophs are located in the upper oxic portion of the soil column they should be more susceptible to changes in air temperature than methanogens in the lower anoxic soil layers. In the FCP studied here where both CH<sub>4</sub> production and oxidation potential are highest in the transition zone, temperature differentials should be small.

**Deleted:** potential

**Deleted:** transition zone

**Deleted:** of

**Deleted:** outcompete

**Deleted:** decrease

**Deleted:** By assuming zero net CH<sub>4</sub> production

**Deleted:** estimated

**Deleted:** temperature profile

**Deleted:** Fig. 7).

oxidation would easily exceed methane production even with an active biomass ratio  $B_{\text{methanotrophs}}/B_{\text{methanogens}}$  lower than 1. A much lower biomass ratio  $B_{\text{methanotrophs}}/B_{\text{methanogens}}$  (0.07-0.26) would make the soil a net source of CH<sub>4</sub>. Studies of functional genes involved in methane production (*mcrA*) and oxidation (*pmoA*) in the active layers in the Western Canadian Arctic region suggested substantial variation in the *pmoA/mcrA* abundance ratio; the range is between  $8.5 \times 10^{-5}$  and  $7.6 \times 10^2$  (Frank-Fahle et al., 2014). Thus, accurate prediction of soil CH<sub>4</sub> production requires quantification of methanogen and methanotroph populations as model constraints. These results suggest the importance of parameterizing the temperature response function and biomass growth function specifically for methanogenesis and methane oxidation in model simulations to determine if the rates of methanogenesis and methane oxidation offset each other. These results support the hypothesis that methanogenesis can be offset by high methane oxidation rates in degraded tundra.

**Deleted:** can still

**Deleted:** CH<sub>4</sub>

**Deleted:** layer of four LCPs

**Deleted:** ;

**Deleted:** Future investigation using molecular methods to quantify

**Deleted:** will provide better

**Deleted:** in the soil column.

The incubations of thawed FCP and HCP soils from all layers revealed substantial differences in the temporal dynamics of CO<sub>2</sub> production. An initial lag was observed from HCP samples at all temperatures, suggesting low initial microbial activity, which might be due to low initial microbial biomass or substrate limitation. In contrast, rapid CO<sub>2</sub> production in FCP soils was observed from both organic layer incubated under oxic conditions and transitional and permafrost layers incubated under anoxic conditions. This temporal pattern of rapid accumulation after thawing was also observed for anaerobic respiration from LCP soils and HCP trough soils (Roy Chowdhury et al., 2015; Yang et al., 2016).

**Deleted:** thawed soil

**Deleted:** moisture content,

**Deleted:** Initial active microbial biomass might also be very low given the low soil water availability.

**Deleted:** active

**Deleted:** transition zone

Coupled iron reduction and organic carbon oxidation processes made substantial contributions to total anaerobic CO<sub>2</sub> production, relative to fermentation and methanogenesis. Acetate was most abundant intermediate and exhibited the most dynamic concentration changes among individual organic acids measured from the soils. Using reaction stoichiometry for acetoclastic methanogenesis and anaerobic respiration through iron reduction (Istok et al., 2010), we estimated the amount of acetate being consumed by these parallel processes in soils from the transition layer and permafrost (Figure 9). In transition layer soils, about half of available acetate was consumed by methanogenesis during the first 20 days of incubation (1.34  $\mu\text{mol g}^{-1}$  out of 2.54  $\mu\text{mol g}^{-1}$ ), while Fe(III) reduction consumed approximately 23% of available acetate (0.60  $\mu\text{mol g}^{-1}$  out of 2.54  $\mu\text{mol g}^{-1}$ ). In contrast, the partitioning of methanogenesis and Fe(III) reduction inverted during 20 to 90 days of anoxic incubation. Methanogenesis and Fe(III) reduction consumed 31% and 59% of available acetate, respectively. Permafrost contained a higher level of available acetate at the beginning of the incubation, and over 60% of the available acetate was rapidly consumed by Fe(III) reduction during the first 20 days of incubation. From 20 to 90 days of incubation, iron reduction still consumed over half of the depleted acetate in the permafrost. This estimate is consistent with our initial characterization of the FCP core, where the soils from the transition layer contained the highest dissolved CH<sub>4</sub> concentrations, and permafrost was associated with significantly higher Fe(II) concentrations (Figure S1). If hydrogen or other organic anions such as formate or propionate were oxidized by methanogens or iron reducers, then estimated acetate production levels would decrease slightly. These simulations indicate that Fe(III) reduction is responsible for most of the acetate mineralized and CO<sub>2</sub> produced in these

**Deleted:** significant

**Deleted:** .

**Deleted:** anaerobic microcosms, which is consistent with previous studies on LCP and HCP carbon decomposition. The consumption of acetate correlated with increases of CH<sub>4</sub> and CO<sub>2</sub> concentrations in previous incubation experiments suggested either acetoclastic methanogenesis or syntrophic acetate oxidation coupled to hydrogenotrophic methanogenesis, which are both consistent with isotopic analyses of CH<sub>4</sub> from the site.

**Deleted:** zone

**Deleted:** Fig. 8

**Deleted:** the

**Deleted:** zone

**Deleted:** , and the number dropped to about 30% during 20 to 90 days of incubation with increasing available acetate pool and increasing Fe(III) reduction.

**Deleted:** potentially

**Deleted:** available

**Deleted:** estimation

**Deleted:** zone

**Deleted:** Fig.

**Deleted:** anaerobic iron respiration could be

soil incubations. As a significant anaerobic respiratory process in Arctic soils, Fe(III) reduction should also be included in CH<sub>4</sub> models to better predict greenhouse gas production in response to a changing climate.

Based on these findings, we propose the following scheme of soil carbon biogeochemistry in the FCP (Figure 10): (1) Increasing temperature facilitates aerobic decomposition of organic carbon in the organic layer, and accelerates anaerobic carbon decomposition in the lower active layer and transition layer through fermentation, iron reduction, and methanogenesis to form CH<sub>4</sub> and CO<sub>2</sub>. (2) CH<sub>4</sub> produced in the transitional and permafrost layers is oxidized close to the site of production or transported to the atmosphere. (3) Fe(III) reduction is the primary anaerobic process responsible for the depletion of acetate, the major SOC decomposition intermediate. In this scheme, the oxic/anoxic interface could dynamically move in the soil column with changes in the water table and pore water distribution. Although the transitional layer contained much less carbon than the permafrost layer, the total carbon loss as the sum of CO<sub>2</sub> and CH<sub>4</sub> was comparable to that from permafrost. Laboratory measurements suggested that acetate accumulated in the organic layer could be transported into deeper layers to support iron reduction and methanogenesis (Yang et al., 2016). This transport might occur through vertical movement of dissolved organic compounds or mixing through cryoturbation (Drake et al., 2015). We will use results from these incubation experiments to structure and parameterize a thermodynamically based microbial growth model that improves simulations of anaerobic organic matter decomposition with CO<sub>2</sub> and CH<sub>4</sub> production.

## 5 Conclusions

Increased warming is predicted to accelerate the transition from wet LCPs to drier FCPs and HCPs in Arctic tundra, which probably function as potential CH<sub>4</sub> sinks. This study demonstrated that CH<sub>4</sub> oxidation capacity was tightly linked to methane availability. Thus, the zone of highest CH<sub>4</sub> oxidation potential is at the suboxic area near the FCP transition layer and the upper permafrost. The measured CH<sub>4</sub> oxidation potential is an order of magnitude higher than the methanogenesis rate. With higher CH<sub>4</sub> residence time in the soil column due to limited gas diffusion in the field, CH<sub>4</sub> oxidation could easily consume CH<sub>4</sub> produced in deep permafrost soil at warming temperature. Given that iron reduction-coupled respiration predominates anaerobic organic carbon decomposition, CO<sub>2</sub> is likely to remain the major form of carbon emission from degraded polygons. This finding provides critical information about the dynamics of CH<sub>4</sub> production and oxidation with increased temperature that need to be incorporated into Arctic terrestrial ecosystem models for better predictions.

## Data availability

The dataset can be found in (Zheng et al., 2017).

Deleted: Fig. 9

Deleted: active

Deleted: zone

Deleted: produce

Deleted: transition zone

Deleted: primary

Deleted: porewater

Deleted: transition zone

Deleted: active

Deleted: atmospheric

Deleted: , rather than O<sub>2</sub> availability in these soils.

Deleted: zone

Deleted: dominates the overall anaerobic processes

#### Author contributions

DG, SW, and BG conceived and organized the research study; TRC, DG and SW collected core samples; JZ, TRC, ZY and performed experiments and acquired data; JZ, TRC and DG analyzed and interpreted data; JZ and DG drafted the manuscript. All authors contributed revisions to the manuscript and have given approval to the final version of the manuscript.

Deleted: analysed

#### 5 Competing interests

The authors declare no competing interests.

#### Acknowledgments

We thank Ji-Won Moon for assistance with ion chromatography, and Bob Busey, Larry Hinzman, Kenneth Lowe and Craig Ulrich for assistance obtaining frozen core samples, as well as UMIAQ, LLC for logistical assistance. The Next-Generation Ecosystem Experiments in the Arctic (NGEE Arctic) project is supported by the Biological and Environmental Research program in the U.S. Department of Energy (DOE) Office of Science. Oak Ridge National Laboratory is managed by UT-Battelle, LLC, for the DOE under Contract No. DE-AC05-00OR22725.

#### References

- 15 Barbier, B. A., Dziduch, I., Liebner, S., Ganzert, L., Lantuit, H., Pollard, W., and Wagner, D.: Methane-cycling communities in a permafrost-affected soil on Herschel Island, Western Canadian Arctic: active layer profiling of *mcrA* and *pmoA* genes, *FEMS Microbiol. Ecol.*, 82, 287-302, <https://doi.org/10.1111/j.1574-6941.2012.01332.x>, 2012.
- Bockheim, J. G.: Importance of cryoturbation in redistributing organic carbon in permafrost-affected soils, *Soil. Sci. Soc. Am. J.*, 71, 1335-1342, <https://doi.org/10.2136/sssaj2006.0414n>, 2007.
- 20 Chang, R. Y.-W., Miller, C. E., Dinardo, S. J., Karion, A., Sweeney, C., Daube, B. C., Henderson, J. M., Mountain, M. E., Eluszkiewicz, J., Miller, J. B., Bruhwiler, L. M. P., and Wofsy, S. C.: Methane emissions from Alaska in 2012 from CARVE airborne observations, *Proc. Natl. Acad. Sci. U.S.A.*, 111, 16694-16699, <https://doi.org/10.1073/pnas.1412953111>, 2014.
- Cheema, S., Zeyer, J., and Henneberger, R.: Methanotrophic and methanogenic communities in Swiss alpine fens dominated by *Carex rostrata* and *Eriophorum angustifolium*, *Appl. Environ. Microbiol.*, 81, 5832-5844, <https://doi.org/10.1128/aem.01519-15>, 2015.
- 25 Christiansen, J. R., Romero, A. J. B., Jørgensen, N. O. G., Glaring, M. A., Jørgensen, C. J., Berg, L. K., and Elberling, B.: Methane fluxes and the functional groups of methanotrophs and methanogens in a young Arctic landscape on Disko Island, West Greenland, *Biogeochemistry*, 122, 15-33, <https://doi.org/10.1007/s10533-014-0026-7>, 2015.
- Commans, R., Landaas, J., Benmergui, J., Luus, K. A., Chang, R. Y.-W., Daube, B. C., Euskirchen, E. S., Henderson, J. M., Karion, A., Miller, J. B., Miller, S. M., Parazoo, N. C., Randerson, J. T., Sweeney, C., Tans, P., Thoning, K., Veraverbeke, S., Miller, C. E., and Wofsy, S. C.: Carbon dioxide sources from Alaska driven by increasing early winter respiration from Arctic tundra, *Proc. Natl. Acad. Sci. U.S.A.*, 114, 5361-5366, <https://doi.org/10.1073/pnas.1618567114>, 2017.
- 30 Dingman, S. L., Barry, R. G., Weller, G., Benson, C., LeDrew, E. F., and Goodwin, C. W.: Climate, snow cover, microclimate, and hydrology, in: *An Arctic ecosystem : the coastal tundra at Barrow, Alaska*, edited by: Brown, J., Miller, P. C., Tieszen, L. L., and Bunnell, F., Dowden, Hutchinson & Ross, Stroudsburg, PA, 30-65, 1980.
- 35 Drake, T. W., Wickland, K. P., Spencer, R. G. M., McKnight, D. M., and Striegl, R. G.: Ancient low-molecular-weight organic acids in permafrost fuel rapid carbon dioxide production upon thaw, *Proc. Natl. Acad. Sci. U.S.A.*, 112, 13946-13951, <https://doi.org/10.1073/pnas.1511705112>, 2015.

- Frank-Fahle, B. A., Yergeau, É., Greer, C. W., Lantuit, H., and Wagner, D.: Microbial Functional Potential and Community Composition in Permafrost-Affected Soils of the NW Canadian Arctic, *PLoS ONE*, 9, e84761, <https://doi.org/10.1371/journal.pone.0084761>, 2014.
- French, H. M.: *The Periglacial Environment*, 3rd ed., John Wiley & Sons, Chichester, 2007.
- Grant, R. F., Mekonnen, Z. A., Riley, W. J., Arora, B., and Torn, M. S.: Mathematical Modelling of Arctic Polygonal Tundra with Ecosystems: Microtopography Determines How CO<sub>2</sub> and CH<sub>4</sub> Exchange Responds to Changes in Temperature and Precipitation, *Journal of Geophysical Research: Biogeosciences*, 122, 3174-3187, <https://doi.org/10.1002/2017JG004037>, 2017.
- Gulledge, J., Doyle, A. P., and Schimel, J. P.: Different NH<sub>4</sub><sup>+</sup>-inhibition patterns of soil CH<sub>4</sub> consumption: A result of distinct CH<sub>4</sub>-oxidizer populations across sites?, *Soil Biol. Biochem.*, 29, 13-21, [https://doi.org/10.1016/S0038-0717\(96\)00265-9](https://doi.org/10.1016/S0038-0717(96)00265-9), 1997.
- Herndon, E. M., Mann, B. F., Roy Chowdhury, T., Yang, Z., Wulfschleger, S. D., Graham, D., Liang, L., and Gu, B.: Pathways of anaerobic organic matter decomposition in tundra soils from Barrow, Alaska, *J. Geophys. Res.-Biogeo.*, 120, 2345-2359, <https://doi.org/10.1002/2015JG003147>, 2015a.
- Herndon, E. M., Yang, Z., Bargar, J., Janot, N., Regier, T. Z., Graham, D. E., Wulfschleger, S. D., Gu, B., and Liang, L.: Geochemical drivers of organic matter decomposition in arctic tundra soils, *Biogeochemistry*, 126, 397-414, <https://doi.org/10.1007/s10533-015-0165-5>, 2015b.
- Hornibrook, E. R. C., Bowes, H. L., Culbert, A., and Gallego-Sala, A. V.: Methanotrophy potential versus methane supply by pore water diffusion in peatlands, *Biogeosciences*, 6, 1491-1504, <https://doi.org/10.5194/bg-6-1491-2009>, 2009.
- Howeler, R. H., and Bouldin, D. R.: The Diffusion and Consumption of Oxygen in Submerged Soils, *Soil. Sci. Soc. Am. J.*, 35, 202-208, <https://doi.org/10.2136/sssaj1971.03615995003500020014x>, 1971.
- Hugelius, G., Strauss, J., Zubrzycki, S., Harden, J. W., Schuur, E. A. G., Ping, C. L., Schirmer, L., Grosse, G., Michaelson, G. J., Koven, C. D., O'Donnell, J. A., Elberling, B., Mishra, U., Camill, P., Yu, Z., Palmtag, J., and Kuhry, P.: Estimated stocks of circumpolar permafrost carbon with quantified uncertainty ranges and identified data gaps, *Biogeosciences*, 11, 6573-6593, <https://doi.org/10.5194/bg-11-6573-2014>, 2014.
- Istok, J. D., Park, M., Michalsen, M., Spain, A. M., Krumholz, L. R., Liu, C., McKinley, J., Long, P., Roden, E., Peacock, A. D., and Baldwin, B.: A thermodynamically-based model for predicting microbial growth and community composition coupled to system geochemistry: Application to uranium bioreduction, *J. Contam. Hydrol.*, 112, 1-14, <https://doi.org/10.1016/j.jconhyd.2009.07.004>, 2010.
- Jørgensen, C. J., Lund Johansen, K. M., Westergaard-Nielsen, A., and Elberling, B.: Net regional methane sink in High Arctic soils of northeast Greenland, *Nature Geosci.*, 8, 20-23, <https://doi.org/10.1038/ngeo2305>, 2015.
- Knoblauch, C., Spott, O., Evgrafova, S., Kutzbach, L., and Pfeiffer, E.-M.: Regulation of methane production, oxidation, and emission by vascular plants and bryophytes in ponds of the northeast Siberian polygonal tundra, *J. Geophys. Res.-Biogeo.*, 120, 2525-2541, <https://doi.org/10.1002/2015JG003053>, 2015.
- Laanbroek, H. J.: Methane emission from natural wetlands: interplay between emergent macrophytes and soil microbial processes. A mini-review, *Annals of botany*, 105, 141-153, <https://doi.org/10.1093/aob/mcp201>, 2010.
- Langford, Z., Kumar, J., Hoffman, F., Norby, R., Wulfschleger, S., Sloan, V., and Iversen, C.: Mapping Arctic Plant Functional Type Distributions in the Barrow Environmental Observatory Using WorldView-2 and LiDAR Datasets, *Remote Sensing*, 8, 733, <https://doi.org/10.3390/rs8090733>, 2016.
- Lara, M. J., McGuire, A. D., Euskirchen, E. S., Tweedie, C. E., Hinkel, K. M., Skurikhin, A. N., Romanovsky, V. E., Grosse, G., Bolton, W. R., and Genet, H.: Polygonal tundra geomorphological change in response to warming alters future CO<sub>2</sub> and CH<sub>4</sub> flux on the Barrow Peninsula, *Glob. Change Biol.*, 21, 1634-1651, <https://doi.org/10.1111/gcb.12757>, 2015.
- Le Mer, J., and Roger, P.: Production, oxidation, emission and consumption of methane by soils: A review, *Eur. J. Soil Biol.*, 37, 25-50, [https://doi.org/10.1016/s1164-5563\(01\)01067-6](https://doi.org/10.1016/s1164-5563(01)01067-6), 2001.
- Lee, H. J., Jeong, S. E., Kim, P. J., Madsen, E. L., and Jeon, C. O.: High resolution depth distribution of Bacteria, Archaea, methanotrophs, and methanogens in the bulk and rhizosphere soils of a flooded rice paddy, *Front. Microbiol.*, 6, <https://doi.org/10.3389/fmicb.2015.00639>, 2015.
- Liebner, S., Schwarzenbach, S. P., and Zeyer, J.: Methane emissions from an alpine fen in central Switzerland, *Biogeochemistry*, 109, 287-299, <https://doi.org/10.1007/s10533-011-9629-4>, 2012.
- Liikanen, A., Huttunen, J. T., Valli, K., and Martikainen, P. J.: Methane cycling in the sediment and water column of mid-boreal hyper-eutrophic Lake Kevätön, Finland, *Ark. Hydrobiol.*, 154, 585-603, <https://doi.org/10.1127/archiv-hydrobiol/154/2002/585>, 2002.
- Liljedahl, A. K., Wilson, C., Kholodov, A., Chamberlain, A., Lee, H., Daanen, R., Cohen, L., Hayes, S., Iwahana, G., Iverson, A., Weiss, T., Hoffman, A., Wulfschleger, S., and Hinzman, L.: Ground Water Levels for NGEE Areas A, B, C and D, Barrow, Alaska, 2012-2014, Accessed at <https://doi.org/10.5440/1183767>, 2015.
- Liljedahl, A. K., Boike, J., Daanen, R. P., Fedorov, A. N., Frost, G. V., Grosse, G., Hinzman, L. D., Iijima, Y., Jorgenson, J. C., Matveyeva, N., Necsoiu, M., Reynolds, M. K., Romanovsky, V. E., Schulla, J., Tape, K. D., Walker, D. A., Wilson, C. J., Yabuki, H., and Zona, D.: Pan-Arctic ice-wedge degradation in warming permafrost and its influence on tundra hydrology, *Nature Geosci.*, 9, 312-318, <https://doi.org/10.1038/ngeo2674>, 2016.

- Lofton, D. D., Whalen, S. C., and Hershey, A. E.: Effect of temperature on methane dynamics and evaluation of methane oxidation kinetics in shallow Arctic Alaskan lakes, *Hydrobiologia*, 721, 209-222, <https://doi.org/10.1007/s10750-013-1663-x>, 2014.
- MacKay, J. R.: Thermally induced movements in ice-wedge polygons, western Arctic coast: a long-term study, *Geographie physique et Quaternaire*, 54, 41-68, <https://doi.org/10.7202/004846ar>, 2000.
- 5 McGuire, A. D., Christensen, T. R., Hayes, D., Heroult, A., Euskirchen, E., Kimball, J. S., Koven, C., Lafleur, P., Miller, P. A., Oechel, W., Peylin, P., Williams, M., and Yi, Y.: An assessment of the carbon balance of Arctic tundra: comparisons among observations, process models, and atmospheric inversions, *Biogeosciences*, 9, 3185-3204, <https://doi.org/10.5194/bg-9-3185-2012>, 2012.
- Parmentier, F. J. W., van Huissteden, J., Kip, N., Op den Camp, H. J. M., Jetten, M. S. M., Maximov, T. C., and Dolman, A. J.: The role of endophytic methane-oxidizing bacteria in submerged *Sphagnum* in determining methane emissions of Northeastern Siberian tundra, *Biogeosciences*, 8, 1267-1278, <https://doi.org/10.5194/bg-8-1267-2011>, 2011.
- 10 Preuss, I., Knoblauch, C., Gebert, J., and Pfeiffer, E. M.: Improved quantification of microbial CH<sub>4</sub> oxidation efficiency in arctic wetland soils using carbon isotope fractionation, *Biogeosciences*, 10, 2539-2552, <https://doi.org/10.5194/bg-10-2539-2013>, 2013.
- Raz-Yaseef, N., Torn, M. S., Wu, Y., Billesbach, D. P., Liljedahl, A. K., Kneafsey, T. J., Romanovsky, V. E., Cook, D. R., and Wullschleger, S. D.: Large CO<sub>2</sub> and CH<sub>4</sub> emissions from polygonal tundra during spring thaw in northern Alaska, *Geophys. Res. Lett.*, 44, 504-513, <https://doi.org/10.1002/2016GL071220>, 2017.
- 15 Riley, W. J., Subin, Z. M., Lawrence, D. M., Swenson, S. C., Torn, M. S., Meng, L., Mahowald, N. M., and Hess, P.: Barriers to predicting changes in global terrestrial methane fluxes: analyses using CLM4Me, a methane biogeochemistry model integrated in CESM, *Biogeosciences*, 8, 1925-1953, <https://doi.org/10.5194/bg-8-1925-2011>, 2011.
- Romanovsky, V. E., and Osterkamp, T. E.: Effects of unfrozen water on heat and mass transport processes in the active layer and permafrost, *Permafrost Periglacial.*, 11, 219-239, [https://doi.org/10.1002/1099-1530\(200007/09\)11:3<219::aid-ppp352>3.0.co;2-7](https://doi.org/10.1002/1099-1530(200007/09)11:3<219::aid-ppp352>3.0.co;2-7), 2000.
- 20 Roslev, P., and King, G. M.: Regulation of methane oxidation in a freshwater wetland by water table changes and anoxia, *FEMS Microbiol. Ecol.*, 19, 105-115, [https://doi.org/10.1016/0168-6496\(95\)00084-4](https://doi.org/10.1016/0168-6496(95)00084-4), 1996.
- Roy Chowdhury, T., Mitsch, W. J., and Dick, R. P.: Seasonal methanotrophy across a hydrological gradient in a freshwater wetland, *Ecol. Eng.*, 72, 116-124, <https://doi.org/http://dx.doi.org/10.1016/j.ecoleng.2014.08.015>, 2014.
- 25 Roy Chowdhury, T., Herndon, E. M., Phelps, T. J., Elias, D. A., Gu, B., Liang, L., Wullschleger, S. D., and Graham, D. E.: Stoichiometry and temperature sensitivity of methanogenesis and CO<sub>2</sub> production from saturated polygonal tundra in Barrow, Alaska, *Glob. Change Biol.*, 21, 722-737, <https://doi.org/10.1111/gcb.12762>, 2015.
- Sachs, T., Giebel, M., Boike, J., and Kutzbach, L.: Environmental controls on CH<sub>4</sub> emission from polygonal tundra on the microsite scale in the Lena river delta, Siberia, *Glob. Change Biol.*, 16, 3096-3110, <https://doi.org/10.1111/j.1365-2486.2010.02232.x>, 2010.
- 30 Sander, R.: Compilation of Henry's law constants (version 4.0) for water as solvent, *Atmos. Chem. Phys.*, 15, 4399-4981, <https://doi.org/10.5194/acp-15-4399-2015>, 2015.
- Schädel, C., Bader, M. K. F., Schuur, E. A. G., Biasi, C., Bracho, R., Capek, P., De Baets, S., Diakova, K., Emakovich, J., Estop-Aragones, C., Graham, D. E., Hartley, I. P., Iversen, C. M., Kane, E., Knoblauch, C., Lupascu, M., Martikainen, P. J., Natali, S. M., Norby, R. J., O'Donnell, J. A., Chowdhury, T. R., Santruckova, H., Shaver, G., Sloan, V. L., Treat, C. C., Turetsky, M. R., Waldrop, M. P., and Wickland, K. P.: Potential carbon emissions dominated by carbon dioxide from thawed permafrost soils, *Nature Clim. Change*, 6, 950-953, <https://doi.org/10.1038/nclimate3054>, 2016.
- 35 Schuur, E. A. G., Bockheim, J., Canadell, J. G., Euskirchen, E., Field, C. B., Goryachkin, S. V., Hagemann, S., Kuhry, P., Lafleur, P. M., Lee, H., Mazhitova, G., Nelson, F. E., Rinke, A., Romanovsky, V. E., Shiklomanov, N., Tarnocai, C., Venevsky, S., Vogel, J. G., and Zimov, S. A.: Vulnerability of permafrost carbon to climate change: implications for the global carbon cycle, *BioScience*, 58, 701-714, <https://doi.org/10.1641/b580807>, 2008.
- 40 Schuur, E. A. G., Abbott, B. W., Bowden, W. B., Brovkin, V., Camill, P., Canadell, J. G., Chanton, J. P., Chapin, F. S., Christensen, T. R., Ciais, P., Crosby, B. T., Czimeczik, C. I., Grosse, G., Harden, J., Hayes, D. J., Hugelius, G., Jastrow, J. D., Jones, J. B., Kleinen, T., Koven, C. D., Krinner, G., Kuhry, P., Lawrence, D. M., McGuire, A. D., Natali, S. M., O'Donnell, J. A., Ping, C. L., Riley, W. J., Rinke, A., Romanovsky, V. E., Sannel, A. B. K., Schädel, C., Schaefer, K., Sky, J., Subin, Z. M., Tarnocai, C., Turetsky, M. R., Waldrop, M. P., Walter Anthony, K. M., Wickland, K. P., Wilson, C. J., and Zimov, S. A.: Expert assessment of vulnerability of permafrost carbon to climate change, *Climatic Change*, 119, 359-374, <https://doi.org/10.1007/s10584-013-0730-7>, 2013.
- 45 Schuur, E. A. G., McGuire, A. D., Schädel, C., Grosse, G., Harden, J. W., Hayes, D. J., Hugelius, G., Koven, C. D., Kuhry, P., Lawrence, D. M., Natali, S. M., Olefeldt, D., Romanovsky, V. E., Schaefer, K., Turetsky, M. R., Treat, C. C., and Vonk, J. E.: Climate change and the permafrost carbon feedback, *Nature*, 520, 171-179, <https://doi.org/10.1038/nature14338>, 2015.
- 50 Segers, R.: Methane production and methane consumption: a review of processes underlying wetland methane fluxes, *Biogeochemistry*, 41, 23-51, <https://doi.org/10.1023/A:100592903>, 1998.
- Shiklomanov, N. I., Streletskiy, D. A., Nelson, F. E., Hollister, R. D., Romanovsky, V. E., Tweedie, C. E., Bockheim, J. G., and Brown, J.: Decadal variations of active-layer thickness in moisture-controlled landscapes, Barrow, Alaska, *J. Geophys. Res.-Biogeo.*, 115, G00104, <https://doi.org/10.1029/2009JG001248>, 2010.
- 55 Shukla, P. N., Pandey, K. D., and Mishra, V. K.: Environmental Determinants of Soil Methane Oxidation and Methanotrophs, *Crit. Rev. Environ. Sci. Technol.*, 43, 1945-2011, <https://doi.org/10.1080/10643389.2012.672053>, 2013.

- Sturtevant, C. S., Oechel, W. C., Zona, D., Kim, Y., and Emerson, C. E.: Soil moisture control over autumn season methane flux, Arctic Coastal Plain of Alaska, *Biogeosciences*, 9, 1423-1440, <https://doi.org/10.5194/bg-9-1423-2012>, 2012.
- Sturtevant, C. S., and Oechel, W. C.: Spatial variation in landscape-level CO<sub>2</sub> and CH<sub>4</sub> fluxes from arctic coastal tundra: influence from vegetation, wetness, and the thaw lake cycle, *Glob. Change Biol.*, 19, 2853-2866, <https://doi.org/10.1111/gcb.12247>, 2013.
- 5 Sundh, I., Nilsson, M., Granberg, G., and Svensson, B. H.: Depth distribution of microbial production and oxidation of methane in northern boreal peatlands, *Microb. Ecol.*, 27, 253-265, <https://doi.org/10.1007/bf00182409>, 1994.
- Throckmorton, H. M., Newman, B. D., Heikoop, J. M., Perkins, G. B., Feng, X., Graham, D. E., O'Malley, D., Vesselinov, V. V., Young, J., Wulfschleger, S. D., and Wilson, C. J.: Active layer hydrology in an arctic tundra ecosystem: quantifying water sources and cycling using water stable isotopes, *Hydrological Processes*, 30, 4972-4986, <https://doi.org/10.1002/hyp.10883>, 2016.
- 10 Treat, C. C., Natali, S. M., Ernakovich, J., Iversen, C. M., Lupascu, M., McGuire, A. D., Norby, R. J., Roy Chowdhury, T., Richter, A., Šantrůčková, H., Schädel, C., Schuur, E. A. G., Sloan, V. L., Turetsky, M. R., and Waldrop, M. P.: A pan-Arctic synthesis of CH<sub>4</sub> and CO<sub>2</sub> production from anoxic soil incubations, *Glob. Change Biol.*, 21, 2787-2803, <https://doi.org/10.1111/gcb.12875>, 2015.
- Vaughn, L. J. S., Conrad, M. E., Bill, M., and Torn, M. S.: Isotopic insights into methane production, oxidation, and emissions in Arctic polygon tundra, *Global change biology*, n/a-n/a, <https://doi.org/10.1111/gcb.13281>, 2016a.
- 15 Vaughn, L. J. S., Conrad, M. E., Bill, M., and Torn, M. S.: Isotopic insights into methane production, oxidation, and emissions in Arctic polygon tundra, *Glob. Change Biol.*, 22, 3487-3502, <https://doi.org/10.1111/gcb.13281>, 2016b.
- von Fischer, J. C., Rhew, R. C., Ames, G. M., Fosdick, B. K., and von Fischer, P. E.: Vegetation height and other controls of spatial variability in methane emissions from the Arctic coastal tundra at Barrow, Alaska, *J. Geophys. Res.-Biogeo.*, 115, G00103, <https://doi.org/10.1029/2009jg001283>, 2010.
- 20 Wainwright, H. M., Dafflon, B., Smith, L. J., Hahn, M. S., Curtis, J. B., Wu, Y., Ulrich, C., Peterson, J. E., Torn, M. S., and Hubbard, S. S.: Identifying multiscale zonation and assessing the relative importance of polygon geomorphology on carbon fluxes in an Arctic tundra ecosystem, *Journal of Geophysical Research: Biogeosciences*, 120, 788-808, <https://doi.org/10.1002/2014JG002799>, 2015.
- Whalen, S. C., and Reeburgh, W. S.: Methane Oxidation, Production, and Emission at Contrasting Sites in a Boreal Bog, *Geomicrobiol. J.*, 17, 237-251, <https://doi.org/10.1080/01490450050121198>, 2000.
- 25 Xu, X., Elias, D. A., Graham, D. E., Phelps, T. J., Carroll, S. L., Wulfschleger, S. D., and Thornton, P. E.: A microbial functional group-based module for simulating methane production and consumption: Application to an incubated permafrost soil, *Journal of Geophysical Research: Biogeosciences*, 120, 1315-1333, <https://doi.org/10.1002/2015JG002935>, 2015.
- Yang, Z., Wulfschleger, S. D., Liang, L., Graham, D. E., and Gu, B.: Effects of warming on the degradation and production of low-molecular-weight labile organic carbon in an Arctic tundra soil, *Soil Biol. Biochem.*, 95, 202-211, <https://doi.org/http://dx.doi.org/10.1016/j.soilbio.2015.12.022>, 2016.
- 30 Yang, Z., Yang, S., Van Nostrand, J. D., Zhou, J., Fang, W., Qi, Q., Liu, Y., Wulfschleger, S. D., Liang, L., Graham, D. E., Yang, Y., and Gu, B.: Microbial community and functional gene changes in Arctic tundra soils in a microcosm warming experiment, *Front. Microbiol.*, 8, 1741, <https://doi.org/10.3389/fmicb.2017.01741>, 2017.
- Zheng, J., RoyChowdhury, T., and Graham, D. E.: CO<sub>2</sub> and CH<sub>4</sub> Production and CH<sub>4</sub> Oxidation in Low Temperature Soil Incubations from Flat- and High-Centered Polygons, Barrow, Alaska, 2012, Accessed at <https://doi.org/10.5440/1288688>, 2017.
- 35 Zona, D., Gioli, B., Commane, R., Lindaas, J., Wofsy, S. C., Miller, C. E., Dinardo, S. J., Dengel, S., Sweeney, C., Karion, A., Chang, R. Y.-W., Henderson, J. M., Murphy, P. C., Goodrich, J. P., Moreaux, V., Liljedahl, A., Watts, J. D., Kimball, J. S., Lipson, D. A., and Oechel, W. C.: Cold season emissions dominate the Arctic tundra methane budget, *Proc. Natl. Acad. Sci. U.S.A.*, 113, 40-45, <https://doi.org/10.1073/pnas.1516017113>, 2016.

Deleted: ¶

Page Break

¶  
 Table 1. Concentrations of Organic Acids\* from FCP Transition Zone and Permafrost  
 ¶

... [3]

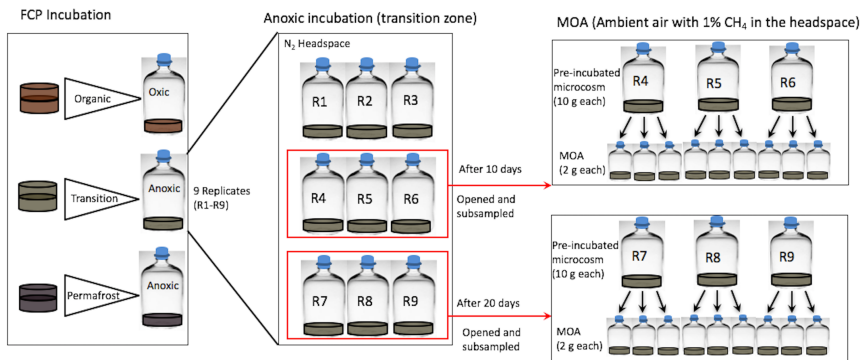


**Figure 1. Soil incubation and methane oxidation assay experimental design. Soils from the transitional layer of a FCP core were used here to illustrate how incubations and methane oxidation assays (MOAs) were constructed at a given temperature. Incubation replicates were destructively sampled after 10 or 20 days to set up MOA with pre-incubated soils. For example, 9 replicate microcosms were created for the FCP transition layer soil, incubated under anoxic conditions. CO<sub>2</sub> and CH<sub>4</sub> in the headspace were cumulatively measured. After 10 days, 3 were opened and subsampled for triplicate MOAs. After 20 days, another 3 were opened and subsampled for triplicate MOAs.**

5

10

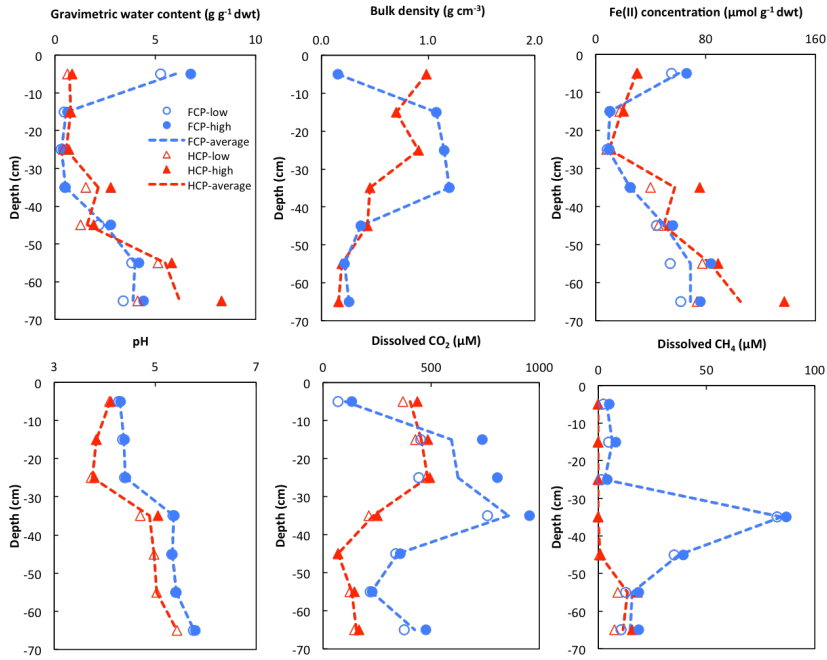


**Figure 2.** Depth profile of gravimetric water content, bulk density, Fe(II) concentration, pH and soil pore water dissolved CO<sub>2</sub> and CH<sub>4</sub> concentrations from FCP (blue) and HCP (red) cores. Replicate measurements were plotted as high and low values in each soil section as blue filled and empty circles (FCP) and red triangles (HCP). Trend lines were plotted based on the average values.

Deleted: averaged value of high and low

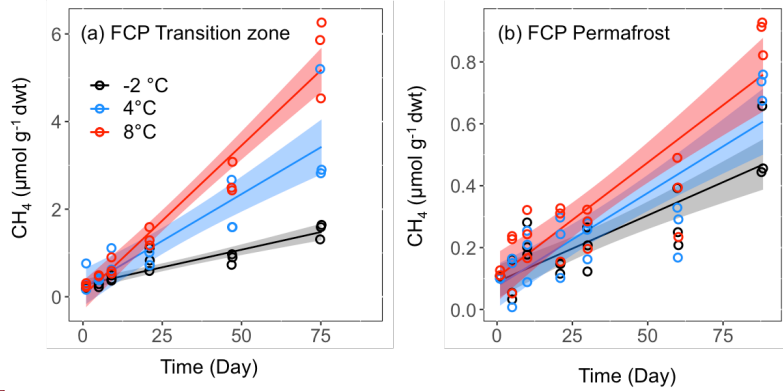
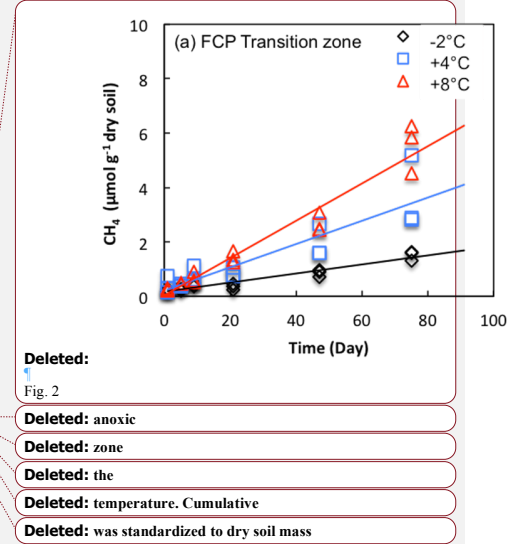


**Figure 3.** CH<sub>4</sub> production in soil microcosms from (a) transition layer, and (b) permafrost layers of FCP at indicated temperatures. The temporal profiles of CH<sub>4</sub> production were best fitted with the linear regression model, and the shaded area represents 95% confidence interval.



Deleted:  
Fig. 2

Deleted: anoxic

Deleted: zone

Deleted: the

Deleted: temperature, Cumulative

Deleted: was standardized to dry soil mass

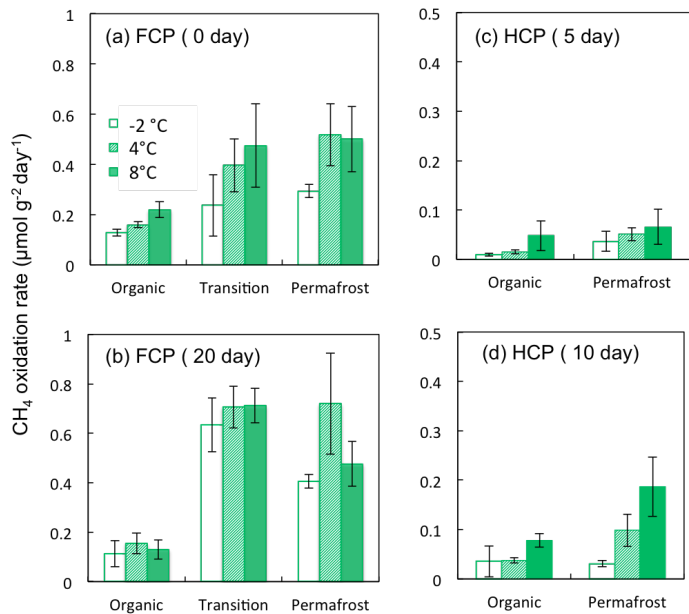
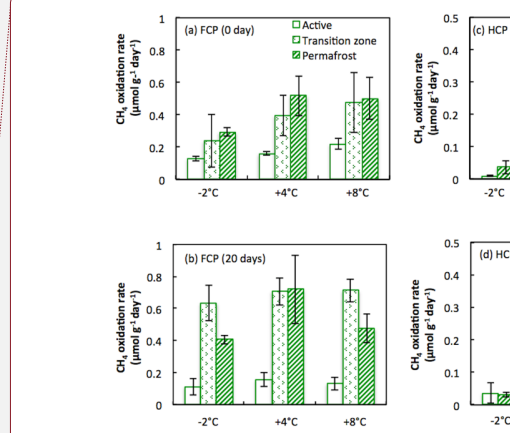


**Figure 4.** CH<sub>4</sub> oxidation potential measured from soils incubated at the indicated temperatures from (a) FCP after 0 days, (b) FCP after 20 days, (c) HCP after 5 days, and (d) HCP after 10 days. Error bars indicate ±1 standard deviation from three replicate incubations.



**Deleted:**  
Fig. 3

**Deleted:** are

**Deleted:** sample

**Deleted:** the mean of

**Deleted:** . Cumulative CH<sub>4</sub> oxidation was standardized to dry soil mass

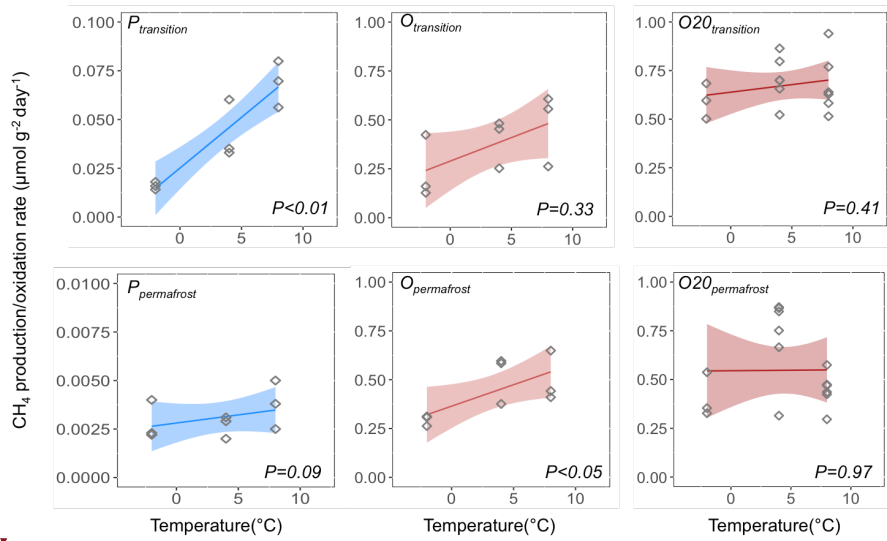
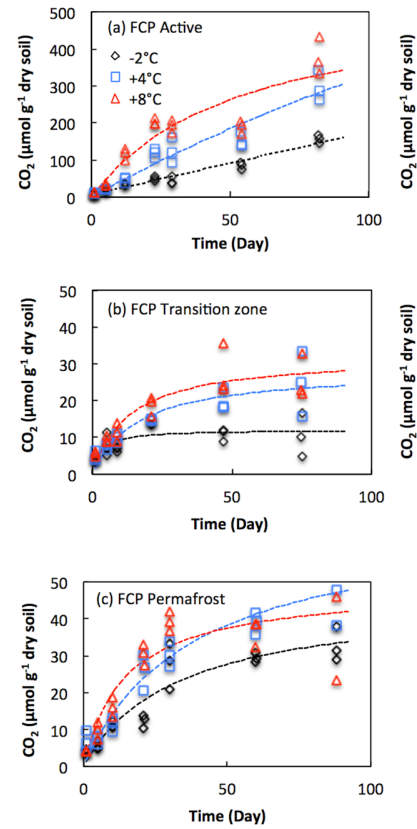


**Figure 5. Temperature sensitivity of  $\text{CH}_4$  production and oxidation measured from the transition and permafrost layers of FCP. Temperature responses of  $\text{CH}_4$  oxidation rates from freshly thawed ( $O_{\text{transition}}$  and  $O_{\text{permafrost}}$ ) and pre-incubated ( $O20_{\text{transition}}$  and  $O20_{\text{permafrost}}$ ) soils were both estimated.**

5



Deleted:  
Fig. 4

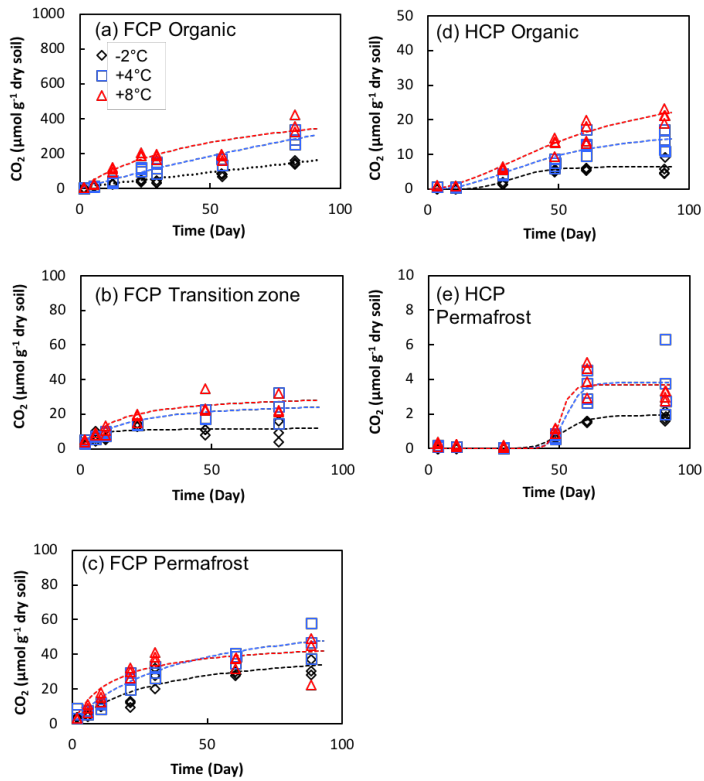
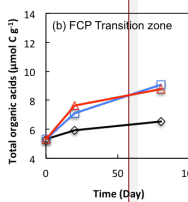
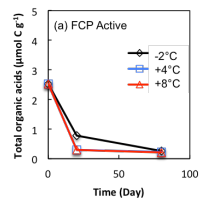


**Figure 6.** Cumulative CO<sub>2</sub> production in soil microcosms from FCP and HCP samples at indicated temperatures.

**Deleted:** (a) active layer, (b) transition zone, and (c) permafrost of the FCP center core and (d) active and (e) permafrost layers of the

**Deleted:** center core. No transition zone was identified in the HCP core.



**Deleted:** Fig. 5

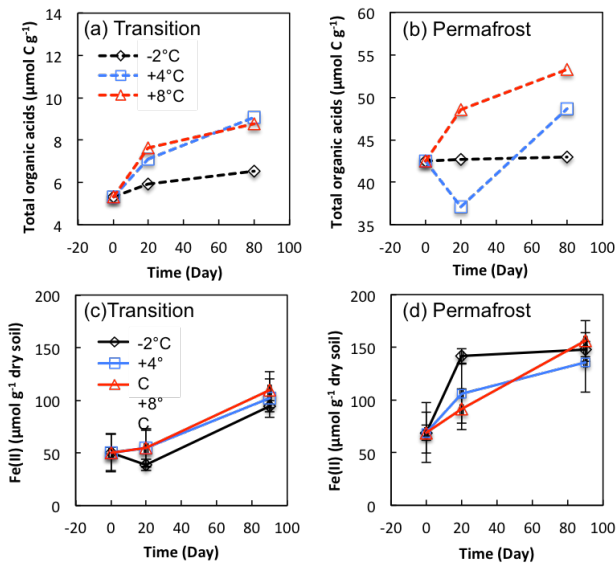
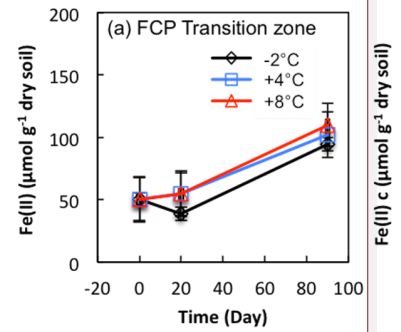


**Figure 7.** Changes in total organic acids, carbon (Top panels) and Fe(II) concentrations (Bottom panels) in soils from transition layer and permafrost of FCP during anoxic incubations. Total organic acids ( $\mu\text{mol C g}^{-1}$ ) were calculated from the concentrations of individual organic acids (Table S5). Error bars for Fe(II) concentrations are  $\pm 1$  standard deviation from three replicate incubations.

Deleted: ( $T_{0.4}$ )  
 Deleted: soil microcosms  
 Deleted: (a) active layer, (b)  
 Deleted: zone  
 Deleted: (c)  
 Deleted: 1).



Deleted:  
 Fig. 6. Changes in Fe(II) concentrations from (a) transition zone and (b) permafrost of FCP during anoxic incubations. Error bars are  $\pm 1$  standard deviation from three replicate incubations.

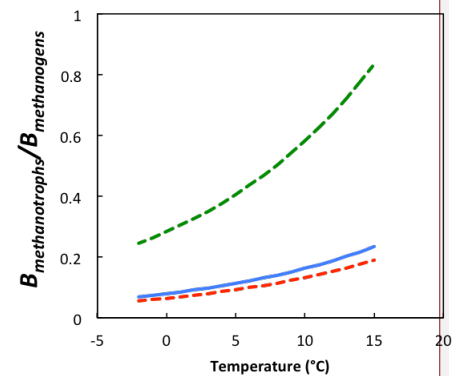


Fig. 7.

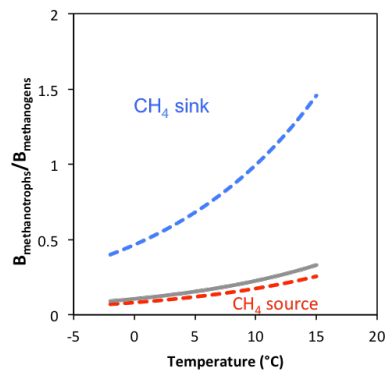
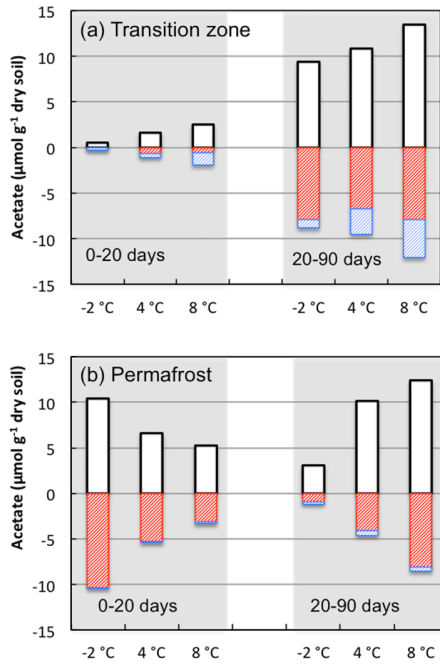


Figure 8. Simulations of active biomass ratio  $B_{\text{methanotrophs}}/B_{\text{methanogens}}$  distribution for Arctic soils to act as  $\text{CH}_4$  sink or source in response to rising temperature. Dissolved  $\text{CH}_4$  and  $\text{O}_2$  concentrations of 0.1 mM in soil pore water are assumed. Half saturation constants ( $K_{m,\text{CH}_4}$  and  $K_{m,\text{O}_2}$ ) represent the baseline value (Grey), high (Blue) and low (Red) range for sensitivity analysis. Biomass ratios below the curves indicate the system could be a  $\text{CH}_4$  source, while biomass ratios above the curves suggest a  $\text{CH}_4$  sink.

5

- Deleted: needed
- Deleted: zero net
- Deleted: emission at different
- Deleted: to be 0.1mM
- Deleted: rates
- Deleted: Blue
- Deleted: Green



**Figure 9. Changes in acetate concentrations associated with production (white bars) and consumption by iron reducing bacteria (red bars) or methanogens (blue bars) were estimated using stoichiometric calculations based on measurements of methane and Fe(II) during incubations from 0 to 20 days and from 20 to 90 days at the indicated incubation temperatures.**

Deleted: Fig. 8. Acetate

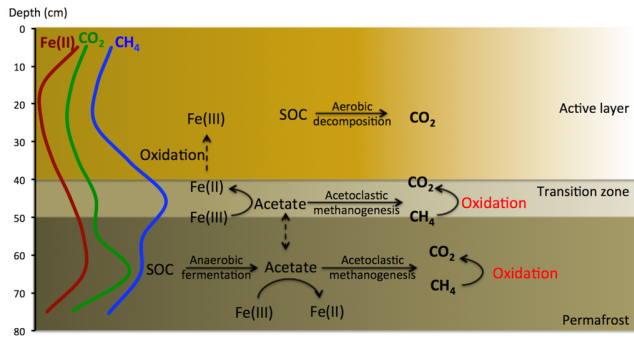


**Figure 10.** Conceptual model of aerobic and anaerobic soil organic carbon decomposition pathways and the release of CO<sub>2</sub> and CH<sub>4</sub> from a flat-centered polygon. Lines on the left marked as Fe(II), CO<sub>2</sub>, and CH<sub>4</sub> represent measurements across the soil column.

**Deleted:** Fig. 9

**Deleted:** qualitative gradients through the soil column. The median height of the water table in FCP centers is at the ground surface, with a standard deviation of ±7 cm during the thaw season .

Pre-incubated soils from FCP microcosms showed similar CH<sub>4</sub> oxidation potentials to newly thawed soils at +8 °C (Fig. 3). However, the potential increased significantly in transition zone samples incubated at -2 °C ( $p=0.01$ ), perhaps due to methanotroph biomass increasing in response to methanogenesis during the 20 day pre-incubation. HCP permafrost layer samples obtained after 10 days of anoxic incubation also show higher CH<sub>4</sub> oxidation potentials ( $p<0.05$ , Fig. 3c, 3d).

### 3.3 Temperature sensitivity of CH<sub>4</sub> production and oxidation

Potential CH<sub>4</sub> production rates from both transition zone and permafrost of FCP were significantly higher at +8 °C than -2 °C ( $p < 0.01$ , t-test). Transition zone soil showed a stronger temperature response, with a Q<sub>10</sub> value of  $4.2 \pm 0.9$ , compared to  $1.7 \pm 0.7$  for permafrost.

The temperature dependency of CH<sub>4</sub> oxidation was consistent among soils layers. CH<sub>4</sub> oxidation potentials significantly increased when the incubation temperature increased from -2 to +8 °C in active layer soil ( $p < 0.01$ ), with a Q<sub>10</sub> value of  $1.7 \pm 0.3$ . Potential rates also increased with temperature for the transition zone and permafrost soils despite more variability: Q<sub>10</sub> values were  $2.0 \pm 1.6$  and  $1.7 \pm 0.5$ , respectively. HCP samples had relatively low rates of CH<sub>4</sub> oxidation. Significant temperature response was observed in pre-incubated permafrost samples from HCP microcosms ( $p=0.01$ ). This soil sample also demonstrated the greatest temperature sensitivity, with a Q<sub>10</sub> value of  $6.1 \pm 1.7$ .

CO<sub>2</sub> production in microcosms of HCP samples showed a different pattern from FCP samples. For active layer soils, the cumulative CO<sub>2</sub> production from aerobic incubations of HCP soils was an order of magnitude lower than FCP soils, despite similar total C content (Fig. 4). The same difference in cumulative CO<sub>2</sub> production was also observed from permafrost incubated under anoxic conditions.

**Table 1.** Concentrations of Organic Acids\* from FCP Transition Zone and Permafrost

	Incubation days	FCP Transition Zone			FCP Permafrost		
		-2°C	4°C	8°C	-2°C	4°C	8°C
Formate	0		0.68			1.68	
	20	0.77	0.72	0.86	1.56	1.43	1.96
	90	0.48±0.06	0.52 ±0.02	0.44 ±0.07	0.99±0.2	1.04±0.24	1.14±0.05
Acetate	0		1.28			10.97	
	20	1.44	1.76	1.89	10.95	9.78	12.94
	90	2.00±0.44	3.10±0.02	3.27±0.07	12.79±1.18	15.29±0.75	16.78±2.92
Propionate	0		0.49			3.82	
	20	0.53	0.65	0.62	3.73	2.97	3.82
	90	0.51±0.12	0.51±0.03	0.39±0.06	8.9±0.33	8.8±0.18	10.1±0.41
Butyrate	0		0.10			1.74	
	20	0.12	0.16	0.20	1.87	1.64	2.13
	90	0.08±0.02	0.15±0.01	0.11±0.03	1.92±0.11	2.11±0.07	2.17±0.13
Oxalate	0		0.09			0.23	
	20	0.12	0.14	0.16	0.28	0.31	0.34
	90	0.10±0.02	0.11±0.00	0.08±0.01	0.23±0.03	0.24±0.03	0.26±0.01

\*Results are presented in  $\mu\text{mol g}^{-1}$  (on a soil dry mass basis). The average and standard deviation are shown for triplicate microcosms incubated for 90 days.

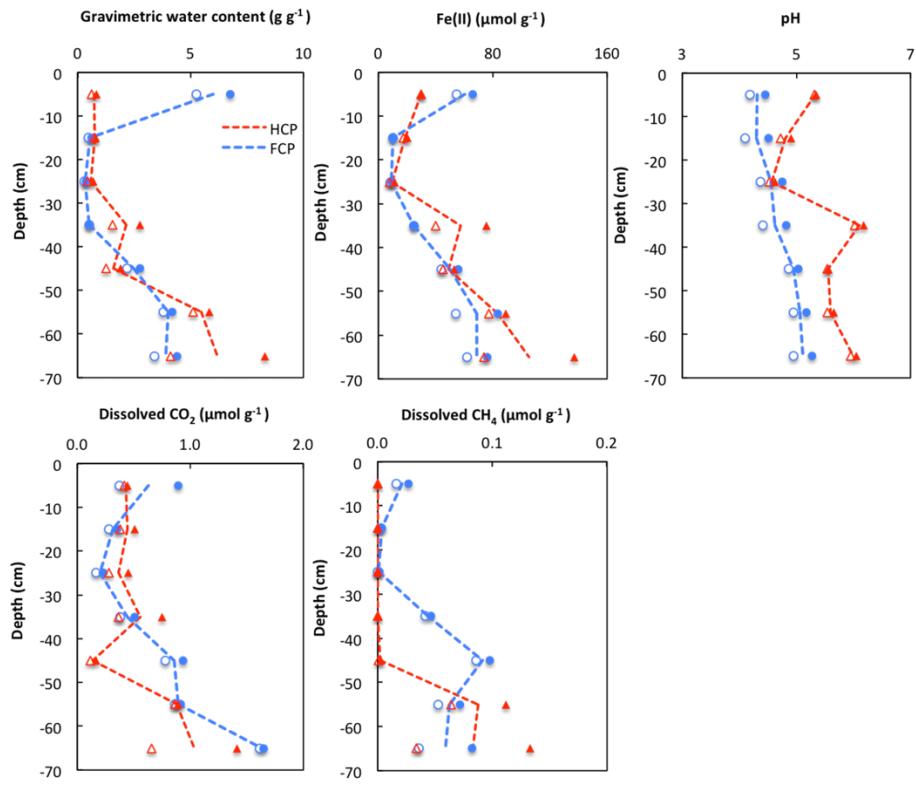


Fig. 1